RECENT RESULTS FROM HERA

Peter Bussey
University of Glasgow

for the H1 and ZEUS Collaborations

A reminder of HERA (1992 – 2007)

For main running, E_e = 27.6 GeV, E_p = 920 GeV

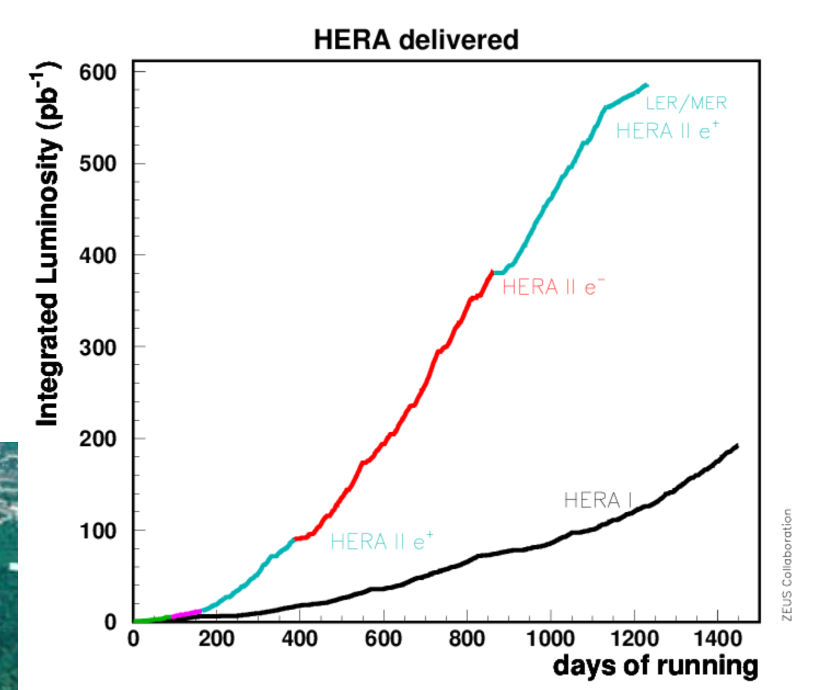

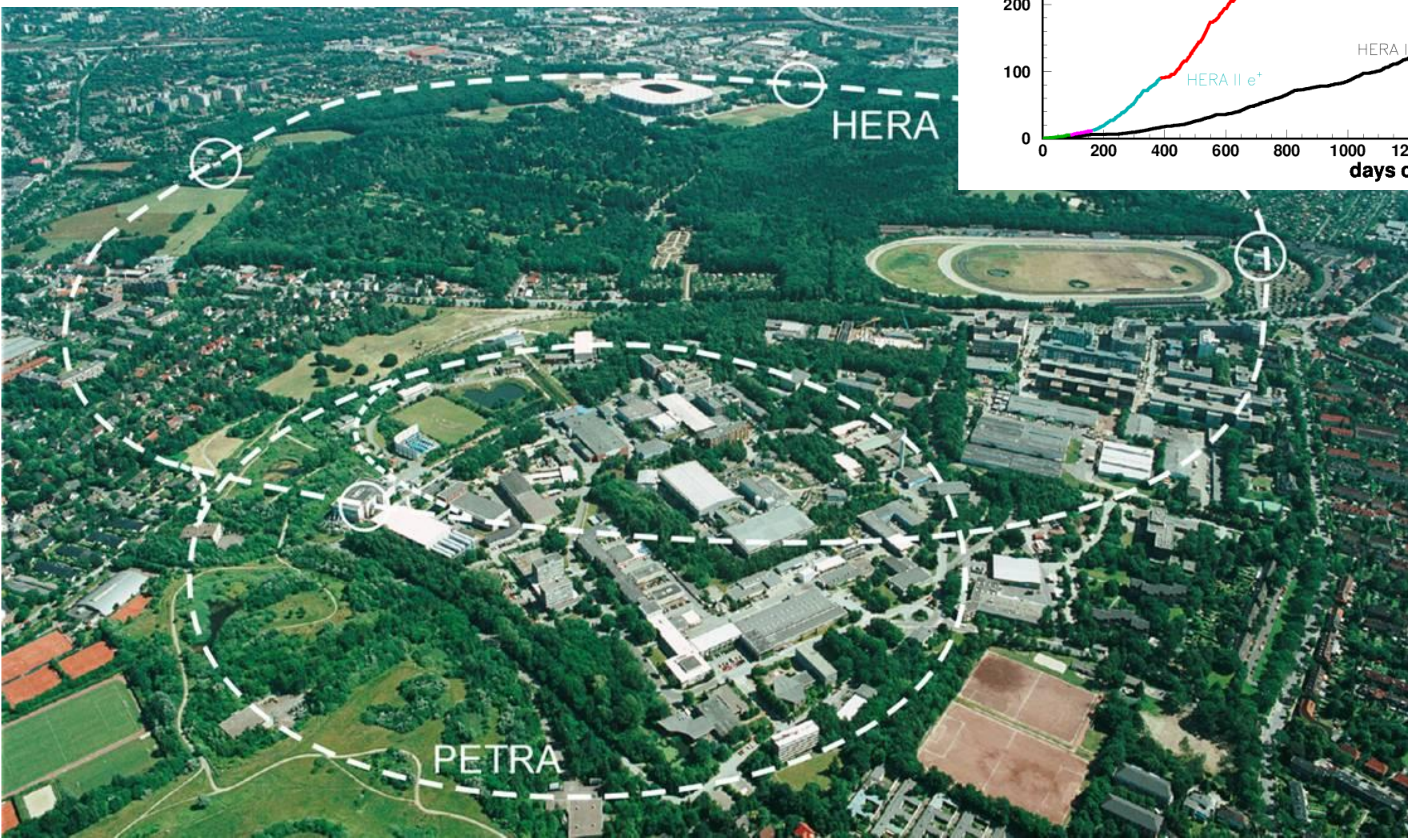

This talk will mainly present diffractive results with one or two extras.

ZEUS:

- **Diffractive prompt photons in photoproduction**
- **Prompt photons plus jets in DIS**
- **Diffractive $\psi(2S)$ and J/ψ production**

H1:

- **Diffractive rho production**
- **Diffractive 4-pi production**
- **Diffractive PDF fit.**

Hard diffractive processes at HERA

Examples of lowest-order resolved–Pomeron diagrams
by which diffractive processes may generate a prompt photon

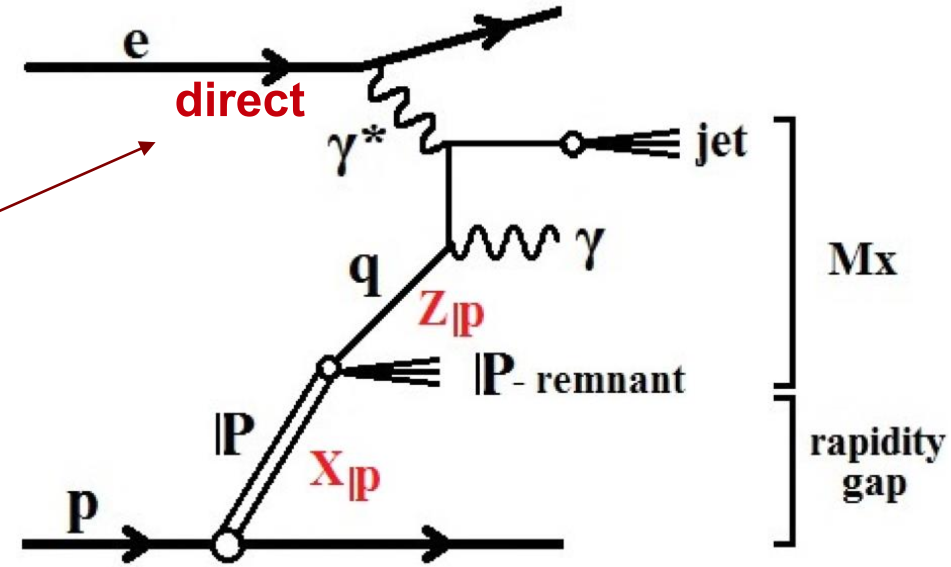

Direct incoming photon gives all its energy to the hard scatter ($x_\gamma = 1$).

Resolved incoming photon gives fraction x_γ of its energy.

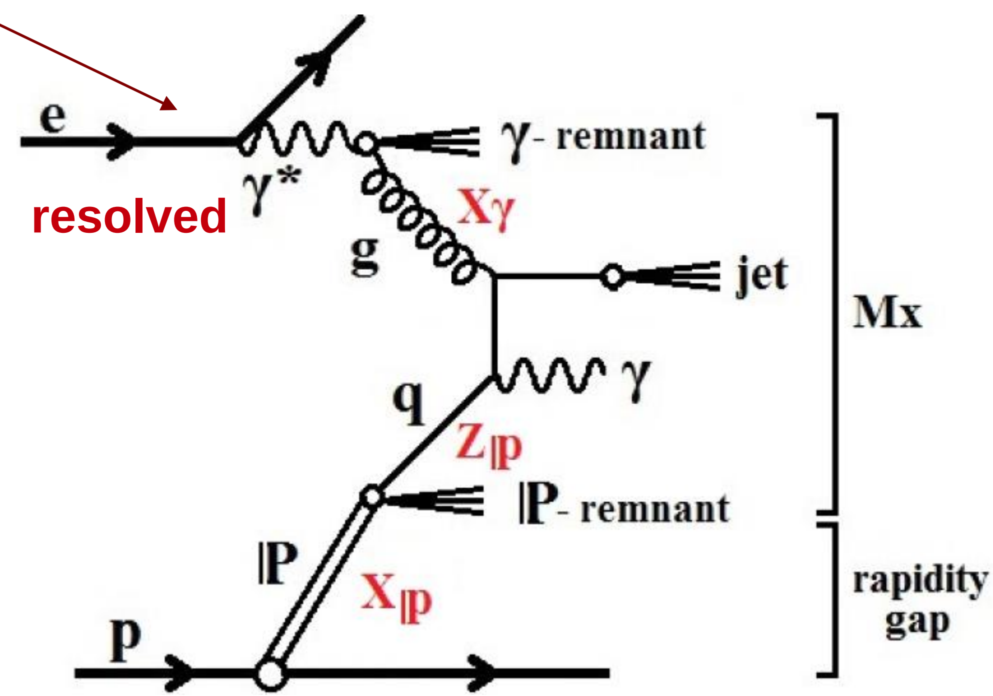

An outgoing photon must couple to a charged particle Line. So the exchanged colourless object ("Pomeron") must have a quark content in this type of diagram.

The proton can also fragment (not shown here).

More kinematics:

x_{IP} = fraction of proton energy taken by Pomeron, measured as

$$\Sigma_{\text{all EFOs}} (E + p_z) \,/\, 2\, E_p$$

z_{IP} = fraction of Pomeron **E+p$_z$** taken by photon + jet measured as

$$\Sigma_{\gamma + \text{jet}}(E + p_z) \,/\, \Sigma_{\text{all EFOs}}(E + p_z)$$

η_{max} = maximum pseudorapidity of observed outgoing particles (E > 0.4 GeV) (ignore forward proton).

Diffractive processes are characterised by a low value of η_{max} and/or low x_{IP}.

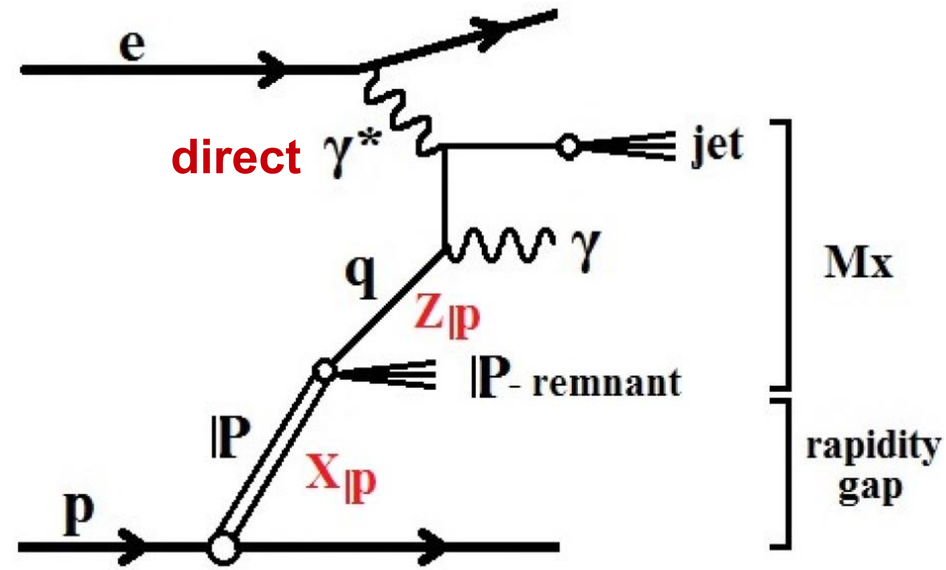

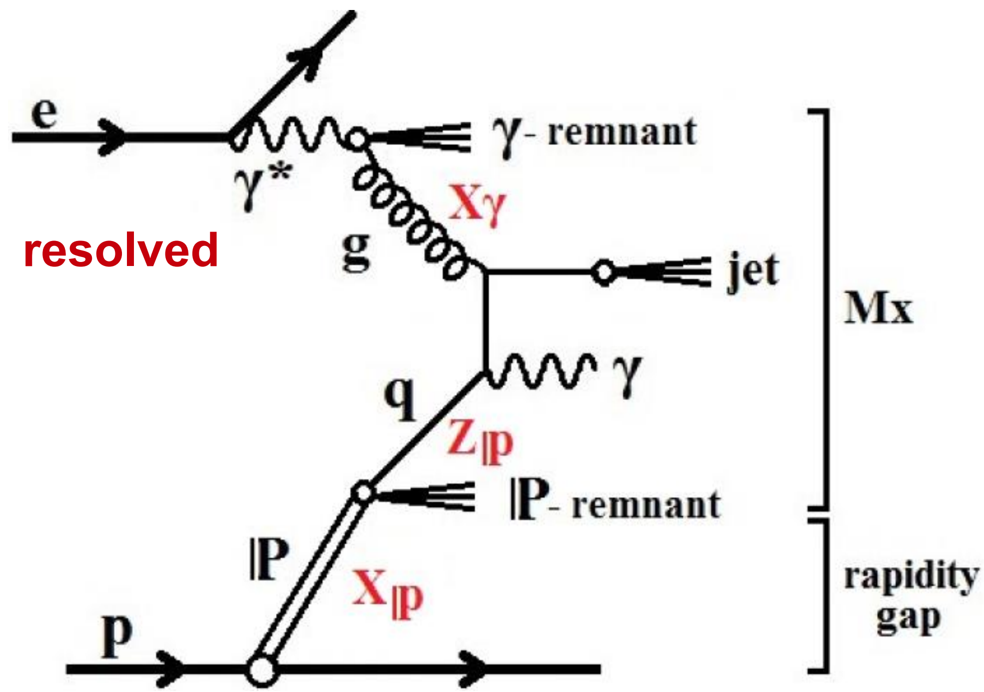

Possible direct Pomeron interactions require a different type of diagram.

e.g.

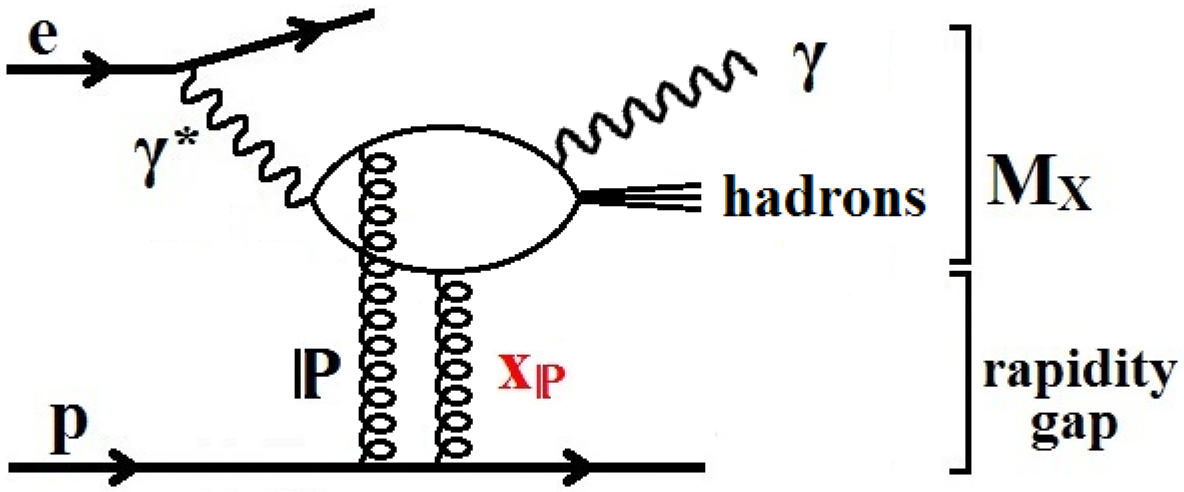

Direct photon + direct Pomeron

Resolved photons also a possibility.

N.B. The proton may become dissociated in diffractive processes

High-p_T photons produced in ep scattering may be:

- Radiated from the incoming or outgoing lepton (LL photons)
- **Produced in a hard partonic interaction (QQ photons)**
- Radiated from a quark in a jet
- Decay product of a hadron in a jet

LL and QQ photons are relatively isolated from other outgoing particles. **QQ usually referred to as "prompt" photons**.

Latest prompt photon results from ZEUS.

Prompt photons in diffractive photoproduction.
Phys. Rev. D 96 (2017) 032006
Deep inelastic scattering, combined variables.
JHEP 1801 (2018) 032

The ZEUS detector

HERA-I data: 1998-2000
HERA-II data: 2004-2007

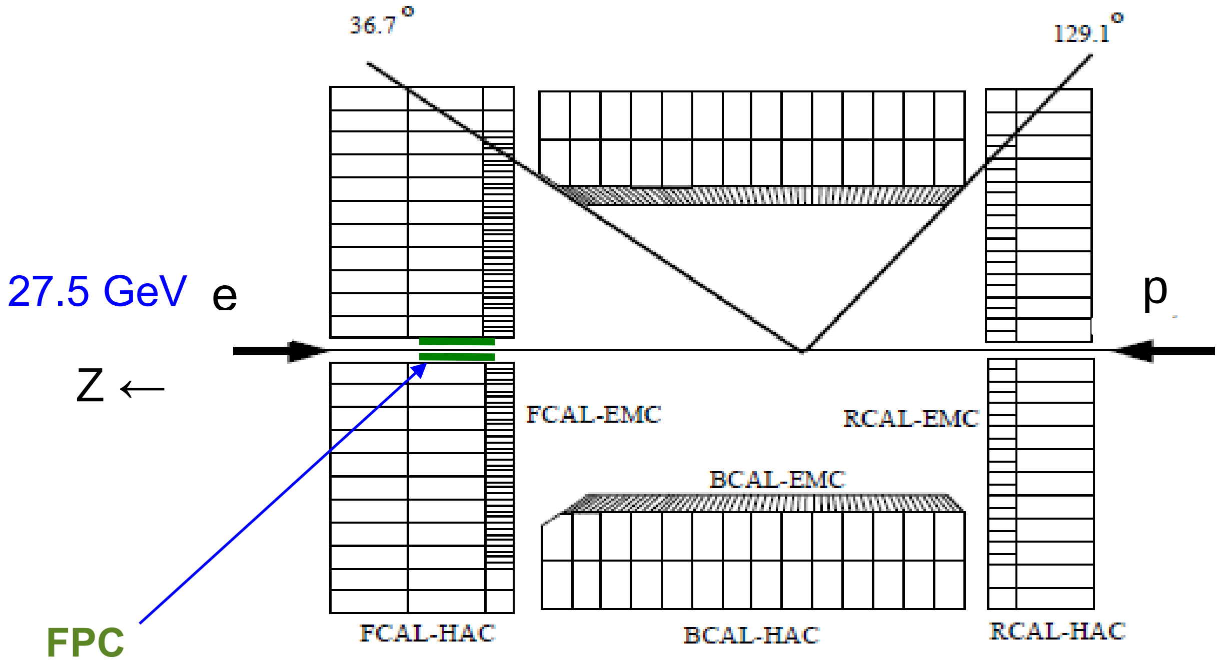

Hard scattered photons are measured in the BCAL, which is finely segmented in the Z direction.

EMC = electromagnetic section

FPC
Forward Plug Calorimeter)
(HERA-I)

Replaced by a beam focussing Magnet In HERA-II

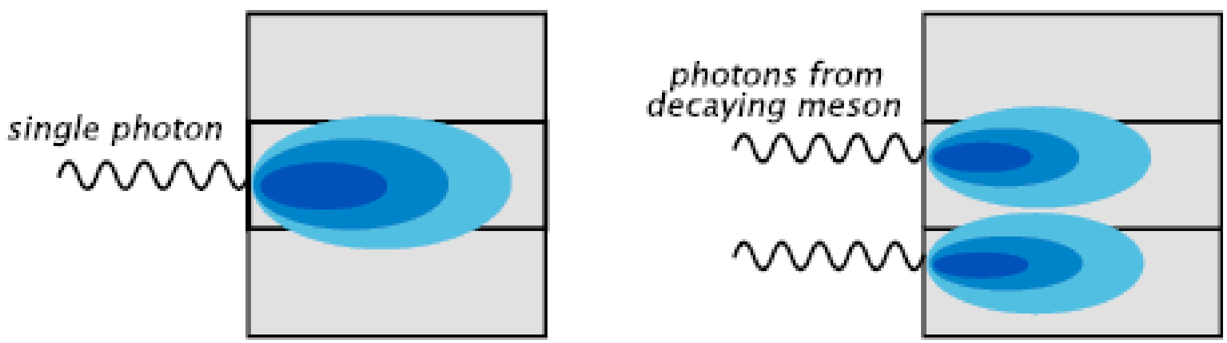

ZEUS prompt photon analyses.

High-energy photon candidate:

- found with energy-clustering algorithm in BCAL: $E_{EMC}/(E_{EMC} + E_{HAD}) > 0.9$
- lower limit imposed on E_T^{γ}
- $-0.7 < \eta^{\gamma} < 0.9$ (i.e. in ZEUS barrel calorimeter)
- **Isolated.** In the “jet” containing the photon candidate, the photon must contain at least 0.9 of the “jet” E_T

Jets

- k_T-cluster algorithm
- $-1.5 < \eta^{jet} < 1.8$
- lower limit imposed on E_T^{jet}

Why we isolate the measured photon:

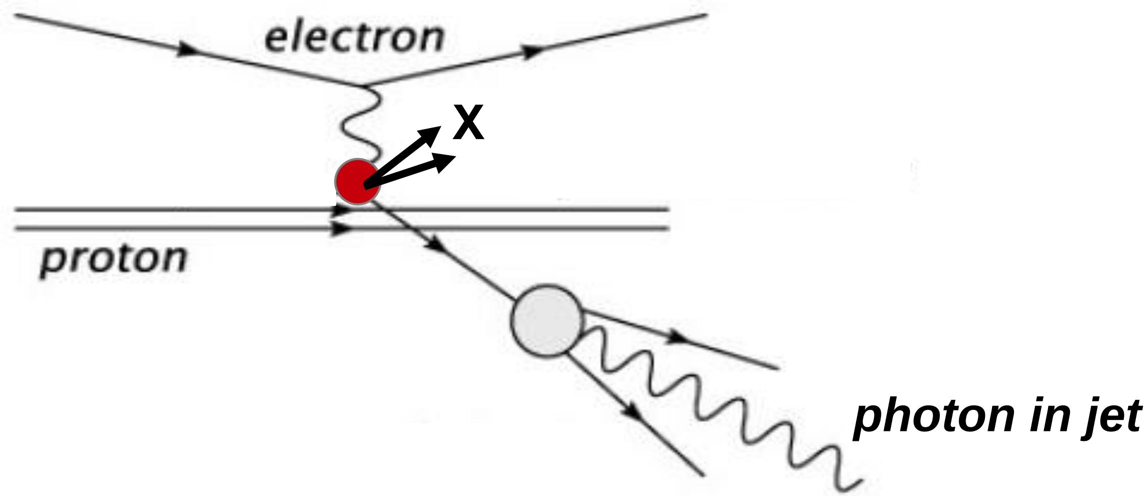

Photons associated with jets require a quark fragmentation function which is not easy to determine – requires non-perturbative input.

Reduce large background from neutral mesons.

Here we measure prompt diffractive photons with and without a jet, using the ZEUS detector, in photoproduction. (i.e small Q^2)

- *Prompt photons emerge directly from the hard scattering process and give a particular view of this.*

- *Allows tests of Pomeron models and explores the non-gluonic aspects of the Pomeron and Pomeron-photon physics in general.*

ZEUS publications of prompt photons in photoproduction:
Phys. Lett. 730 (2014) 293   JHEP 08 (2014) 03

H1 on inclusive diffractive prompt photons in photoproduction:
Phys. Lett. 672 (2009) 219

Diffractive photoproduced dijets:
(H1) Eur. Phys. J. 6 ((1999) Eur. Phys. J. 421, 70 (2008)15
(ZEUS) Eur. Phys. J 55 (2008) 171

ZEUS diffractive analysis.

1) The forward scattered proton is not measured in these analyses.

2) Non-diffractive events are characterised by a forward proton shower.
   To remove them, require $\eta_{max} < 2.5$ and $x_{IP} < 0.03$
   η_{max} is evaluated from ZEUS energy flow objects (EFOs), which combine tracking and calorimeter cluster information.

3) A cut $0.2 < y_{JB} < 0.7$ removes most DIS events.

4) Remove remaining DIS events and Bethe-Heitler and DVCS events (γ e) by excluding events with identified electron or ≤ 5 EFOs

5) Remaining non-diffractive events neglected, could be 0-10% of our cross sections. Treated as a systematic.

6) **HERA I** data: use the FPC to remove more non-diffractive background. It also suppressed many proton dissociation events.

   Use HERA-I data to measure total cross section. 82 pb^{-1}
   Use HERA-II data to study shapes of distributions. 374 pb^{-1}

Monte Carlo simulation

Uses the **RAPGAP** generator
(H. Jung Comp Phys Commun 86 (1995) 147)

Based on leading order parton-level QCD matrix elements.

Some higher orders are modelled by initial and final state leading-logarithm parton showers.

Fragmentation uses the Lund string model as implemented in PYTHIA.

The H1 2006 DPDF fit B set is used to describe the density of partons in the diffractively scattered proton.
For resolved photons, the SASGAM-2D pdf is used.

Fit the x_γ distribution to direct-photon and resolved-photon RAPGAP components.

A 70:30 mixture is found and used throughout.

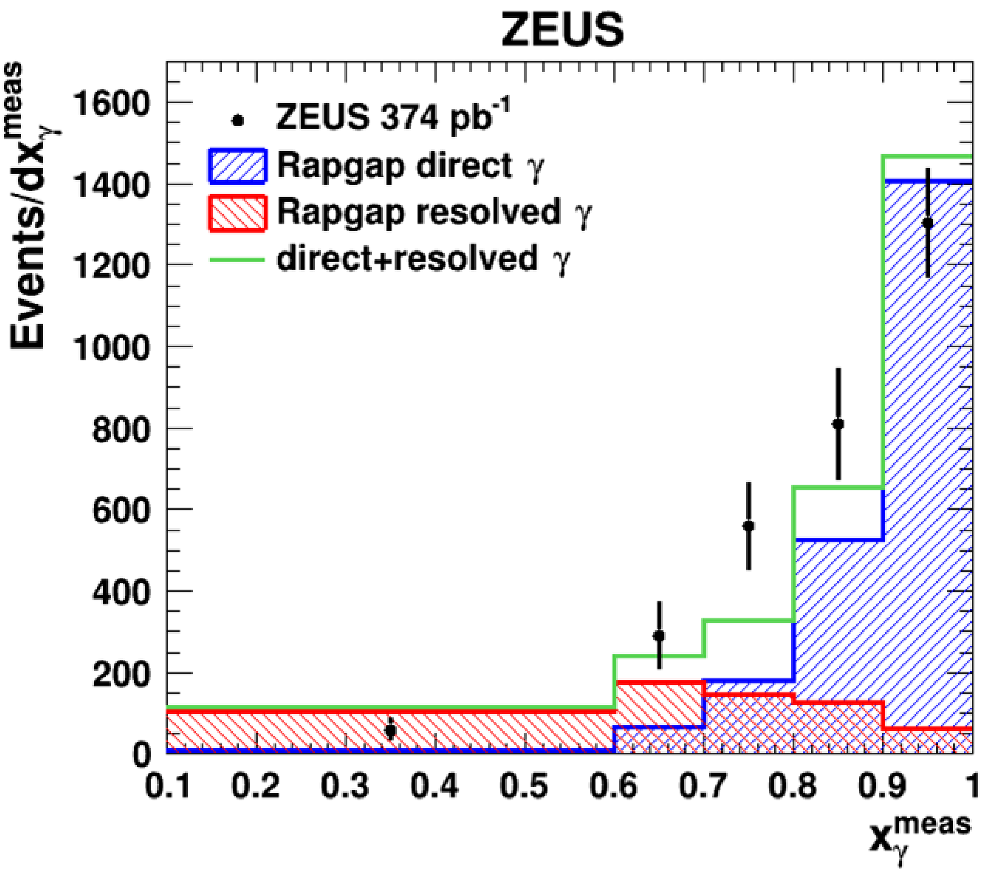

$$x_\gamma^{meas} = \Sigma_{\gamma + jet}(E - p_z) / \Sigma_{all\ EFOs}(E - p_z)$$

Results

Cross sections compared to RAPGAP normalised to total observed cross section. Inner error bar is statistical. Outer (total) includes correlated normalisation and non-diffractive subtraction uncertainty.

Transverse energy of photon.

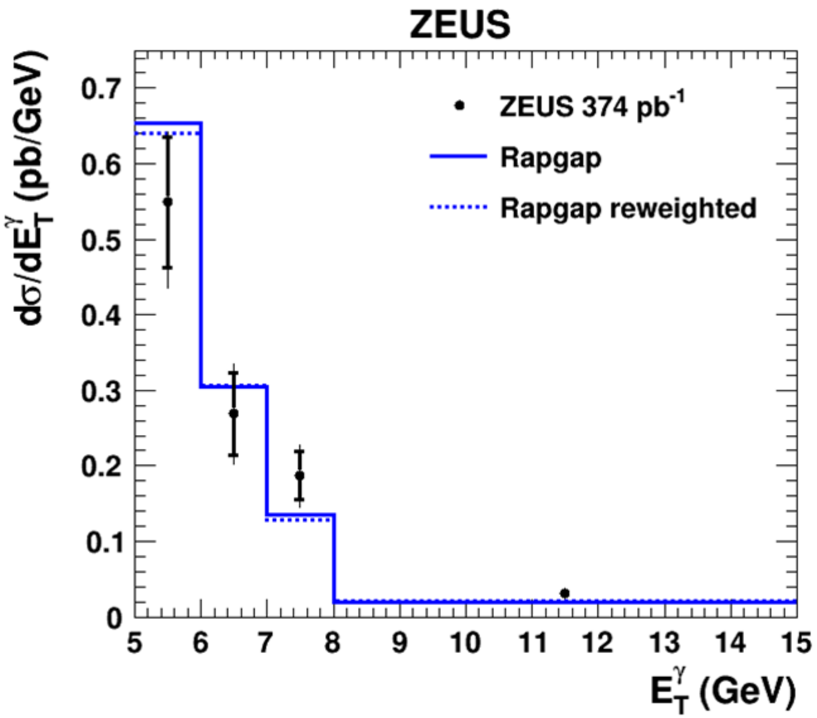

Inclusive photon

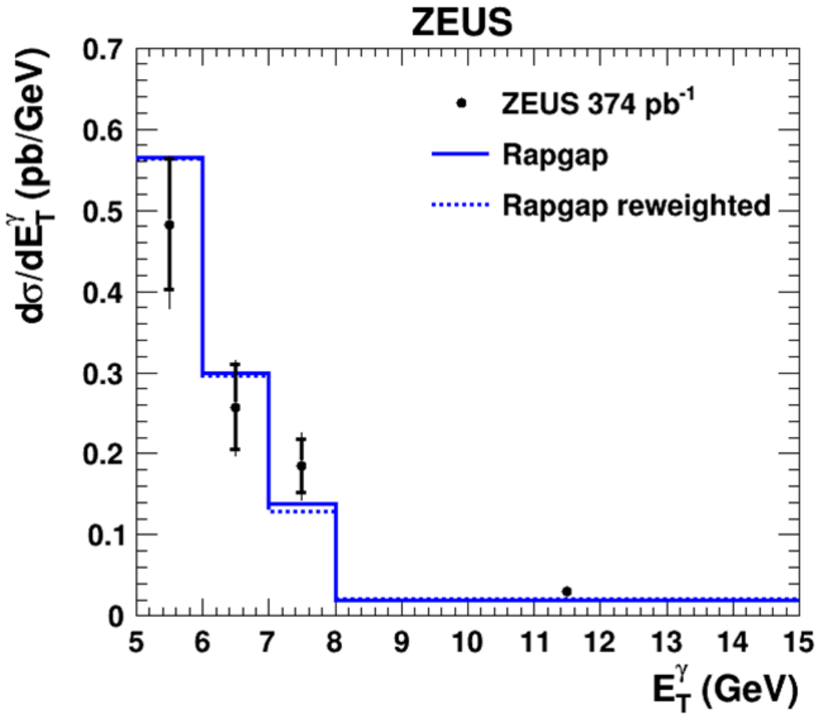

Photon + jet with E_T > 4 GeV

Shape of data well described by Rapgap. **Most photons are accompanied by a jet.**

Cross section in $z_{IP}^{meas} = \Sigma_{\gamma + jet}(E + p_z) / \Sigma_{all\ EFOs}(E + p_z)$

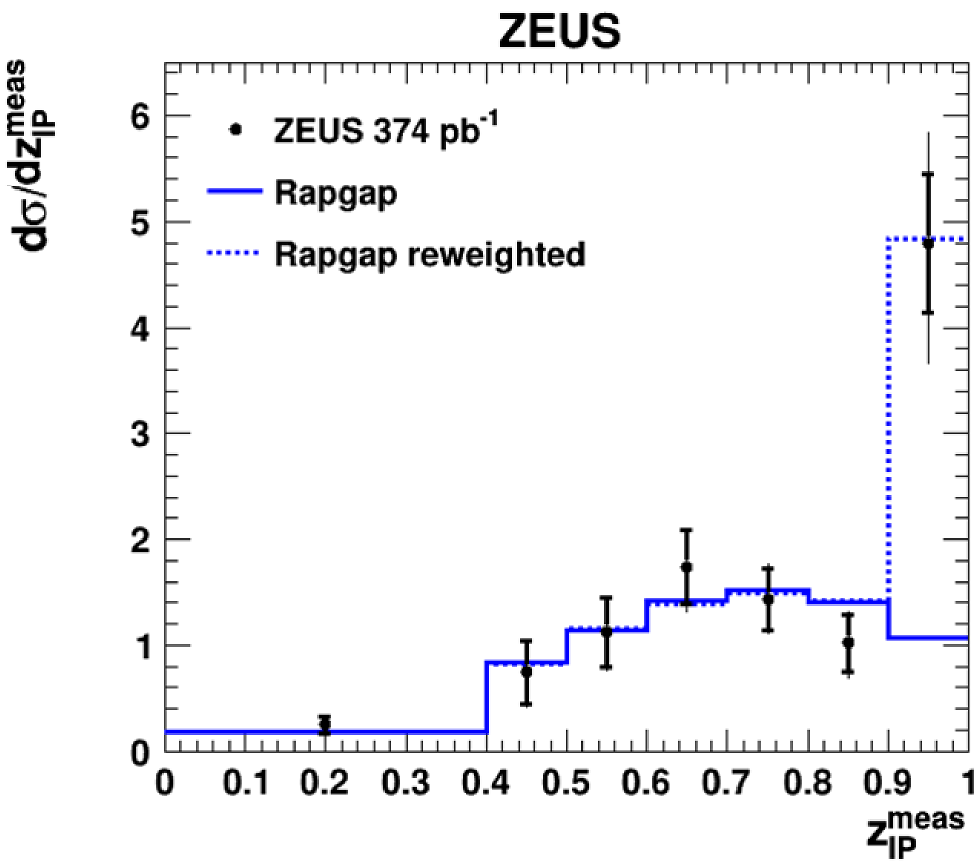

Evidence for direct Pomeron interactions

Photon-electron events have been removed.
(ep → epγ)

Other backgrounds estimated and found to be at a low level

Using HERA-I data, integrated cross section for z_{IP}^{meas} **< 0.9** = $0.68 \pm 0.14\ ^{+0.06}_{-0.07}$ pb

Rapgap gives 0.68 pb. No allowance for proton dissociation which is ~ 16 ± 4%.

Cross sections for region $z_{IP}^{meas} < 0.9$ Rapgap is normalised to data in this region.

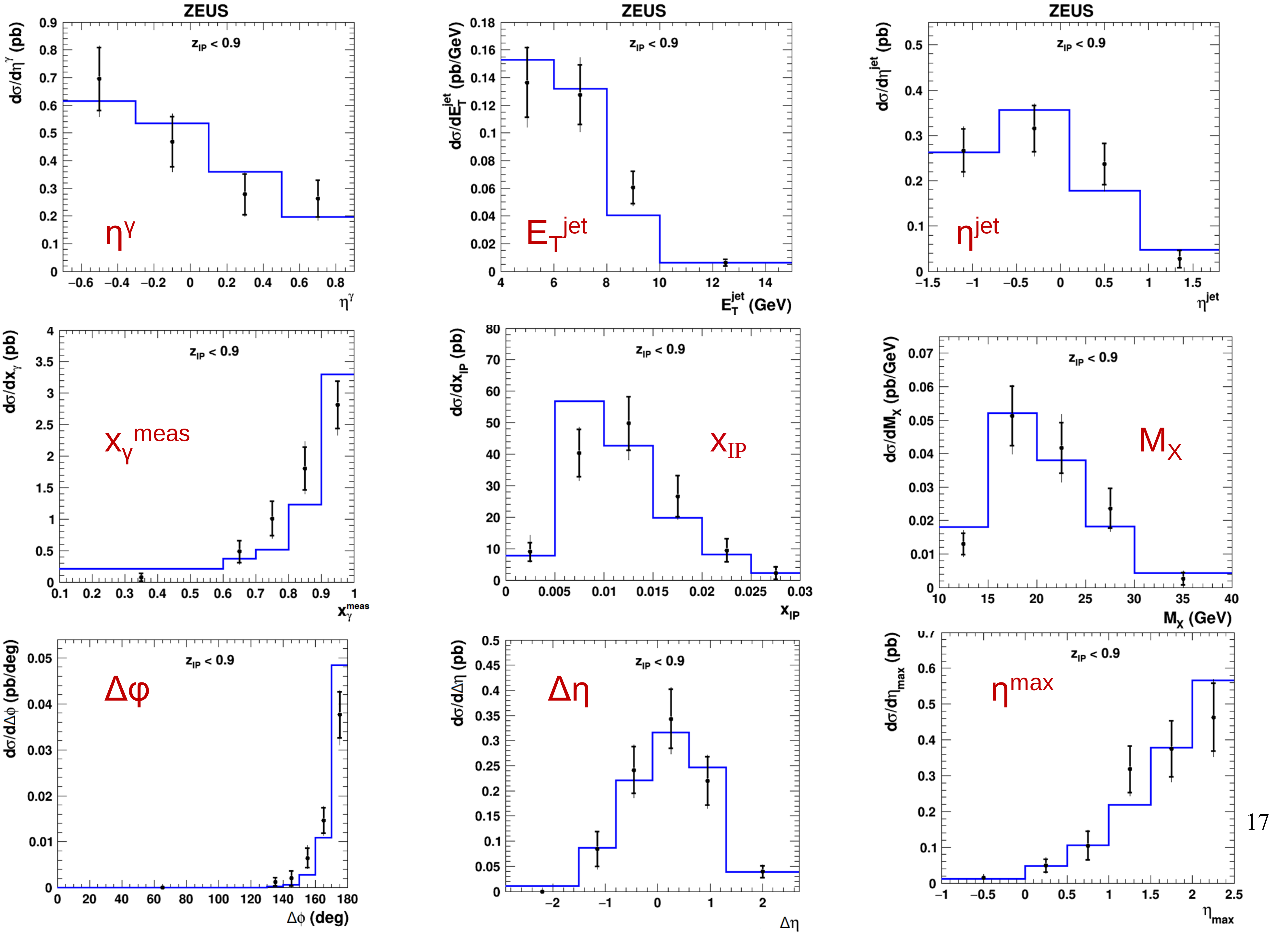

Cross sections for region $z_{IP}^{meas} \geq 0.9$ Rapgap is normalised to data in this region.

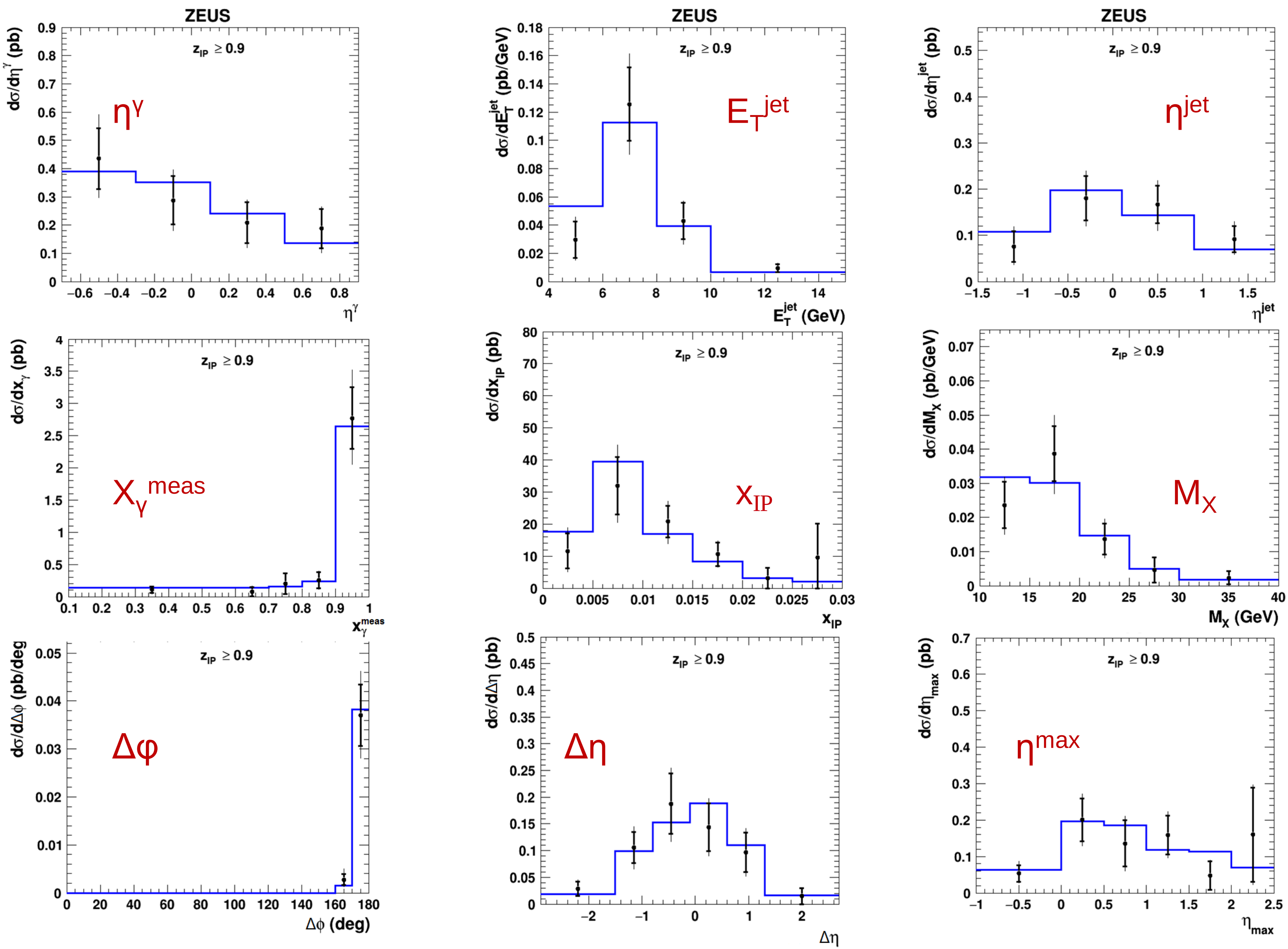

Conclusions

Diffractive results were defined by cuts on η_{max} and x_{IP}

Most of the detected photons are accompanied by a jet.

The variable z_{IP}^{meas} shows a peak at high values that gives evidence for a direct-Pomeron process not modelled by RAPGAP

In both regions of z_{IP}^{meas} , cross sections of kinematic variables are well described in shape by **Rapgap**, confirming a common set of PDFs in diffractive DIS (where they were evaluated) and photoproduction at $z_{IP}^{meas} < 0.9$.

DIS analysis of event structures in prompt photons + jet.

Main further selections:

$4 < E_T^{\gamma} < 15$ GeV

$E_T^{jet} > 2.5$ GeV

$10 < Q^2 < 350$ GeV^2

Plotted "combined" parameters:

- $x_{\gamma}^{meas} = \frac{\sum_{jet,\gamma}(E-p_z)}{2y_{JB}E_e}$
- $x_{p}^{obs} = \frac{\sum_{jet,\gamma}(E+p_z)}{2E_p}$

- $\Delta\eta = \eta_{jet} - \eta_{\gamma}$
- $\Delta\varphi = \varphi_{jet} - \varphi_{\gamma}$
- $\Delta\varphi_{e,\gamma} = \varphi_e - \varphi_{\gamma}$
- $\Delta\eta_{e,\gamma} = \eta_e - \eta_{\gamma}$

Width of BEMC photon candidate

Fit for number of photons in each measured bin.

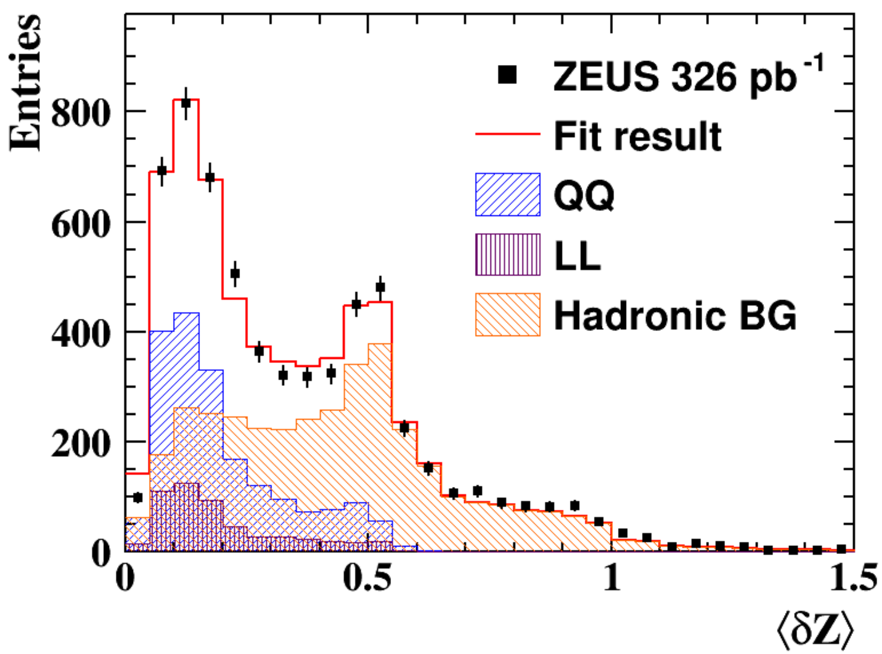

Results for full Q2 range, compared to PYTHIA*1.6 (QQ) + HERACLES (LL)

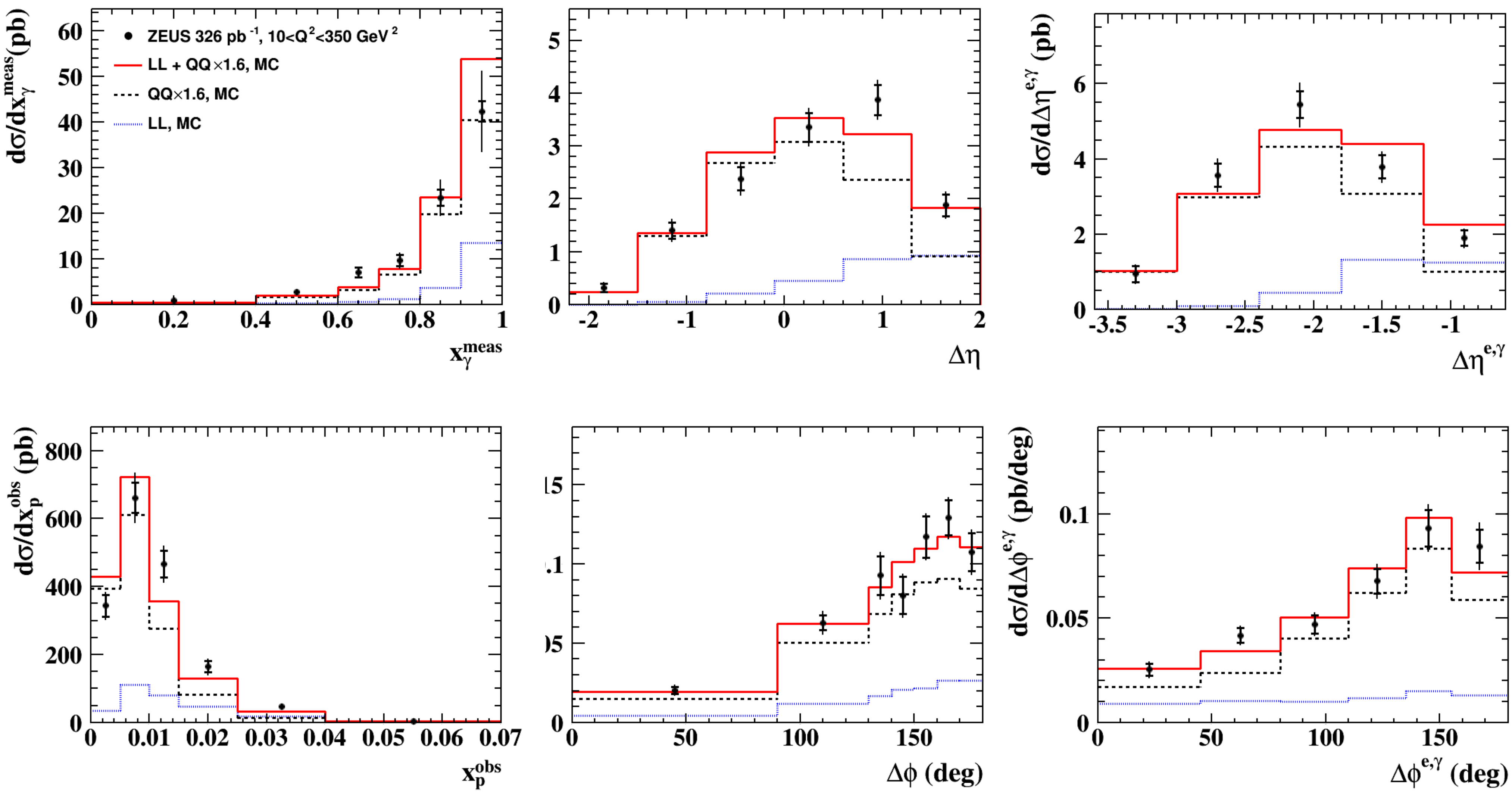

A reasonable description is obtained.

AFG: Aurenche, Fontannaz and Guillet : EPJ C44 (2005) 395 NLO

BLZ: Baranov, Lipatov and Zotov: PRD81 (2010) 094034 kT-factorisation

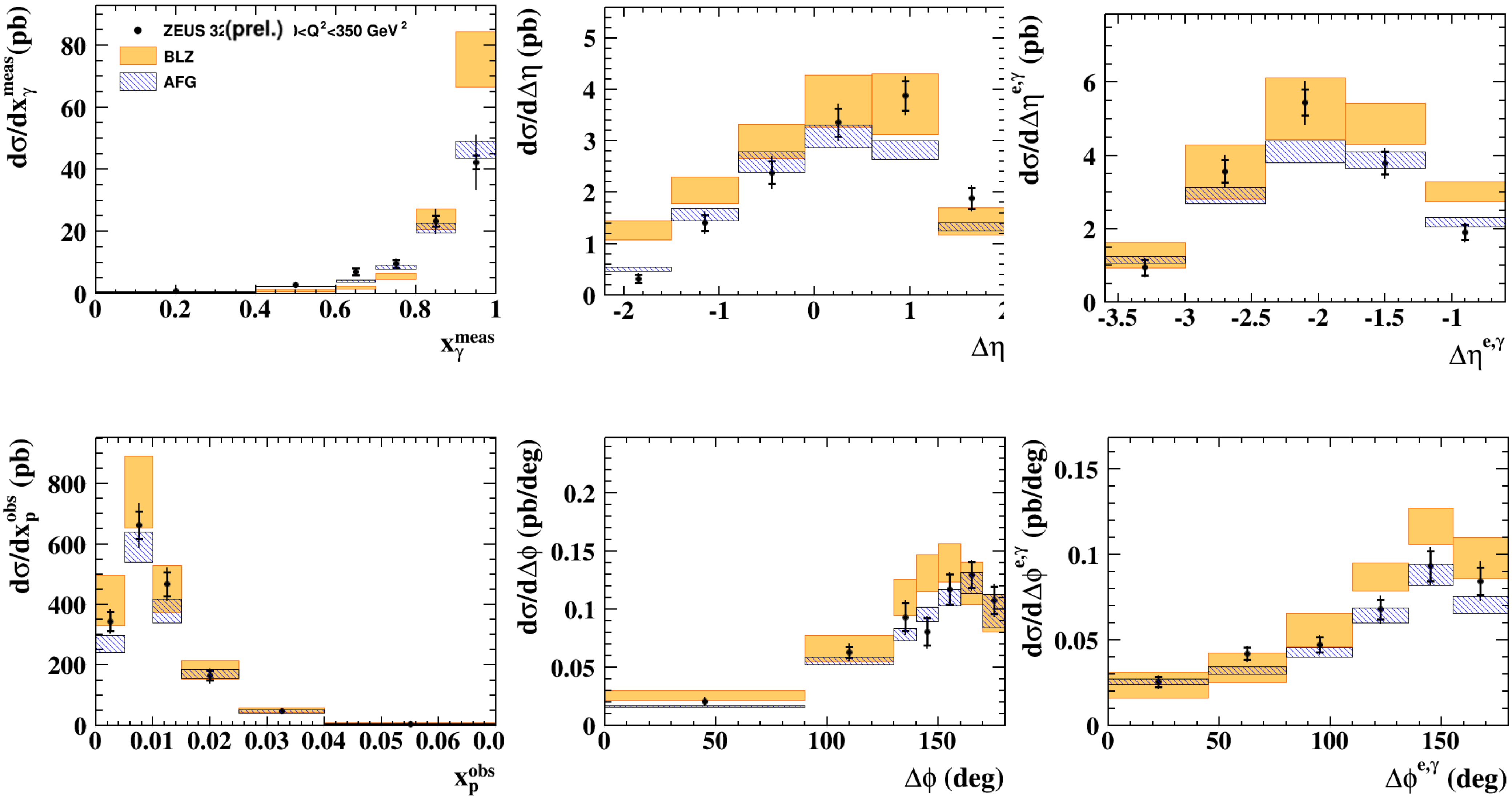

AFG is better, especially for x_γ, though not perfect here.

Conclusions

DIS: results are in better agreement with AFG model than with BLZ but agree well, after rescaling, with Pythia + Heracles/Ariadne

ZEUS: Measurement of the ψ(2S) to J/ψ cross-section ratio in photoproduction

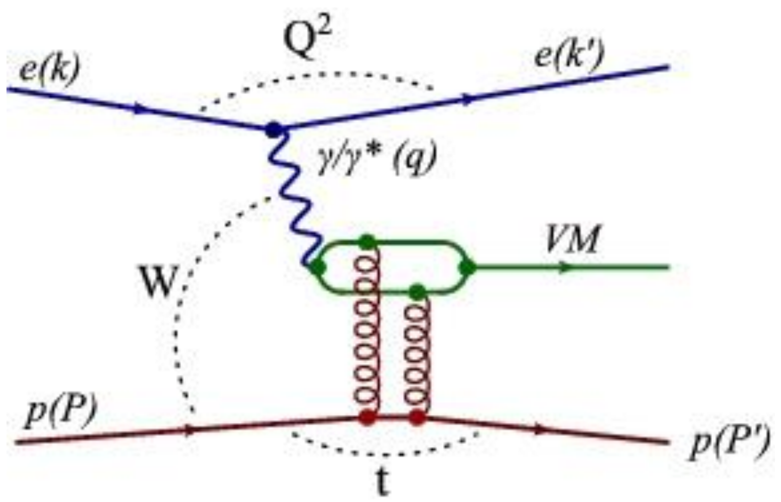

Detect ψ(2S) and J/ψ
using muonic decays

Motivation:

The two VM states have different radial wavefunctions, giving sensitivity to theoretical modelling.

C.f. ZEUS DIS study:
Nucl. Phys. B909 (2016) 934

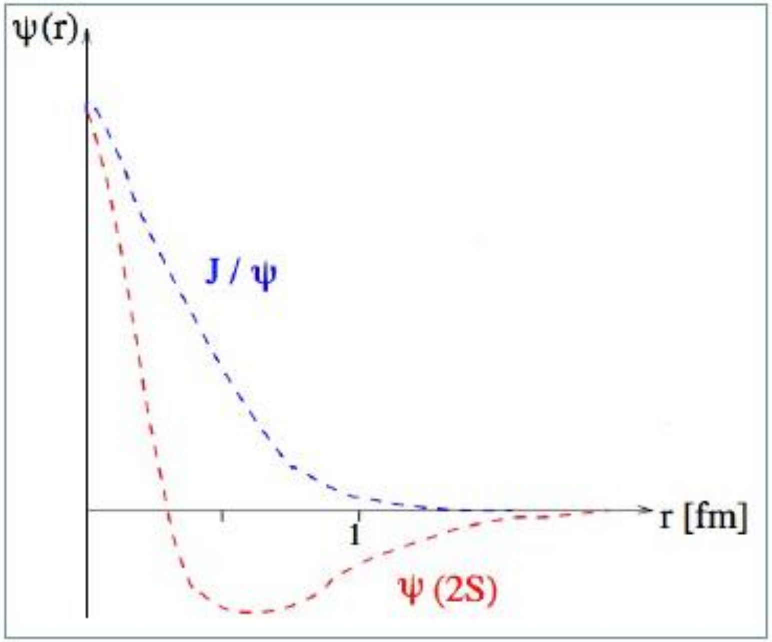

Detect **J/ψ** using $\mu^+\mu^-$ final state

Detect **ψ(2S)** using $\mu^+\mu^-$ final state (2-prong) and
and $\mu^+\mu^- \pi^+\pi^-$ final state (4-prong)
with **$\psi(2S) \rightarrow J/\psi^- \pi^+\pi^-) \rightarrow \mu^+\mu^- \pi^+\pi$**

2-prong final states: exclusive muon trigger
2 tracks, p_T > 100 MeV/c
>1 muon identification, both min. ionising in calorimeter
cosmic rejection

4-prong final states: 4 tracks, two with the muon conditions
pion candidates have pT > 120 MeV/c
no explicit cosmic rejection
$2.8 < M(\mu^+\mu)^- < 3.4$ GeV for J/ψ^-selection

Mont Carlos: DIFFVM for the signals, and **GRAPE** for backgrounds.

Dimuon masses in three W ranges show expected peaks.

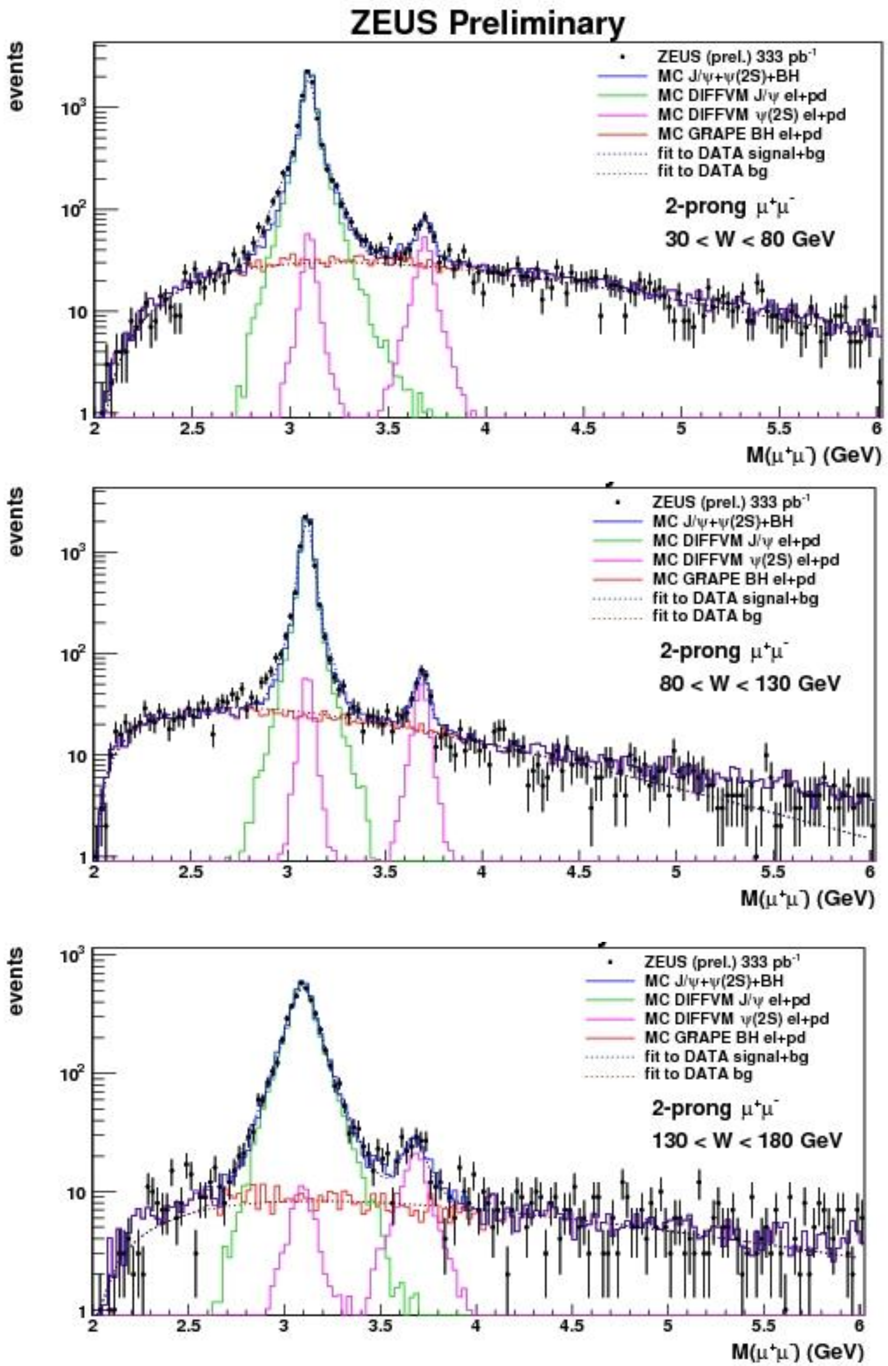

μ$^+$μ$^-$ π$^+$π- mass shows good peak

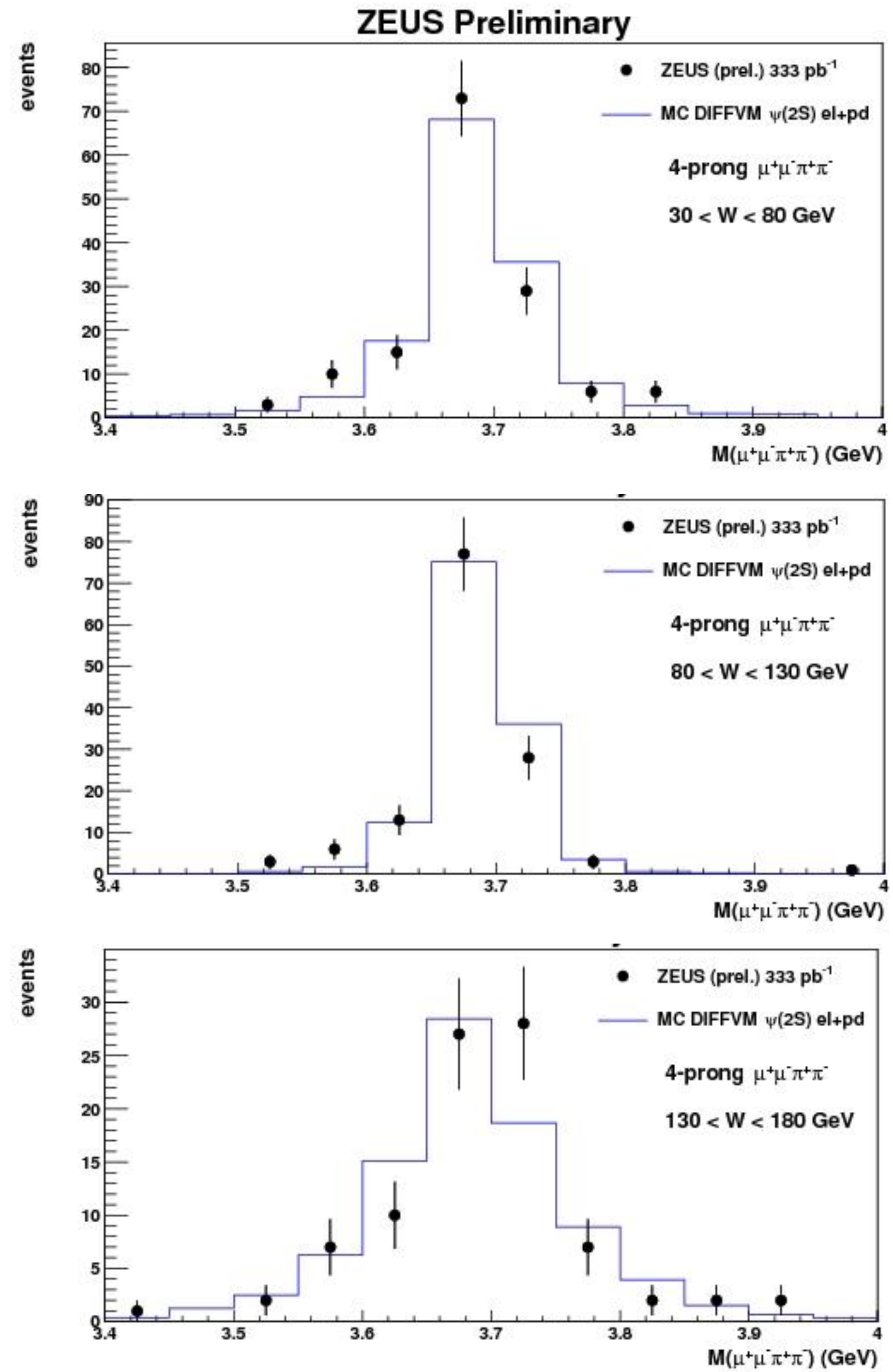

Results for ratio of the
ψ(2S) /J/ψ
Integrated cross sections

Little or no variation with W.

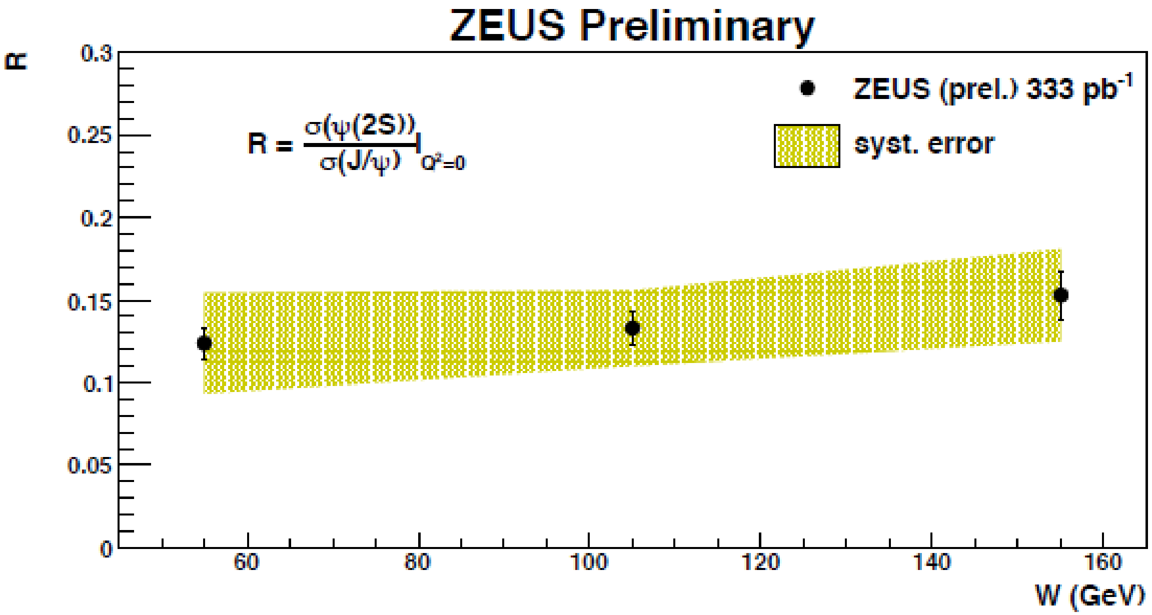

Branching ratios used:

$$BR(\psi(2S) \to J/\psi\pi^+\pi^-) = (34.49 \pm 0.3)\%,$$
$$BR(\psi(2S) \to \mu^+\mu^-) = (7.9 \pm 0.9) \times 10^{-3},$$
$$BR(J/\psi \to \mu^+\mu^-) = (5.961 \pm 0.033)\%$$

Comparison with other results for different photon virtualities.

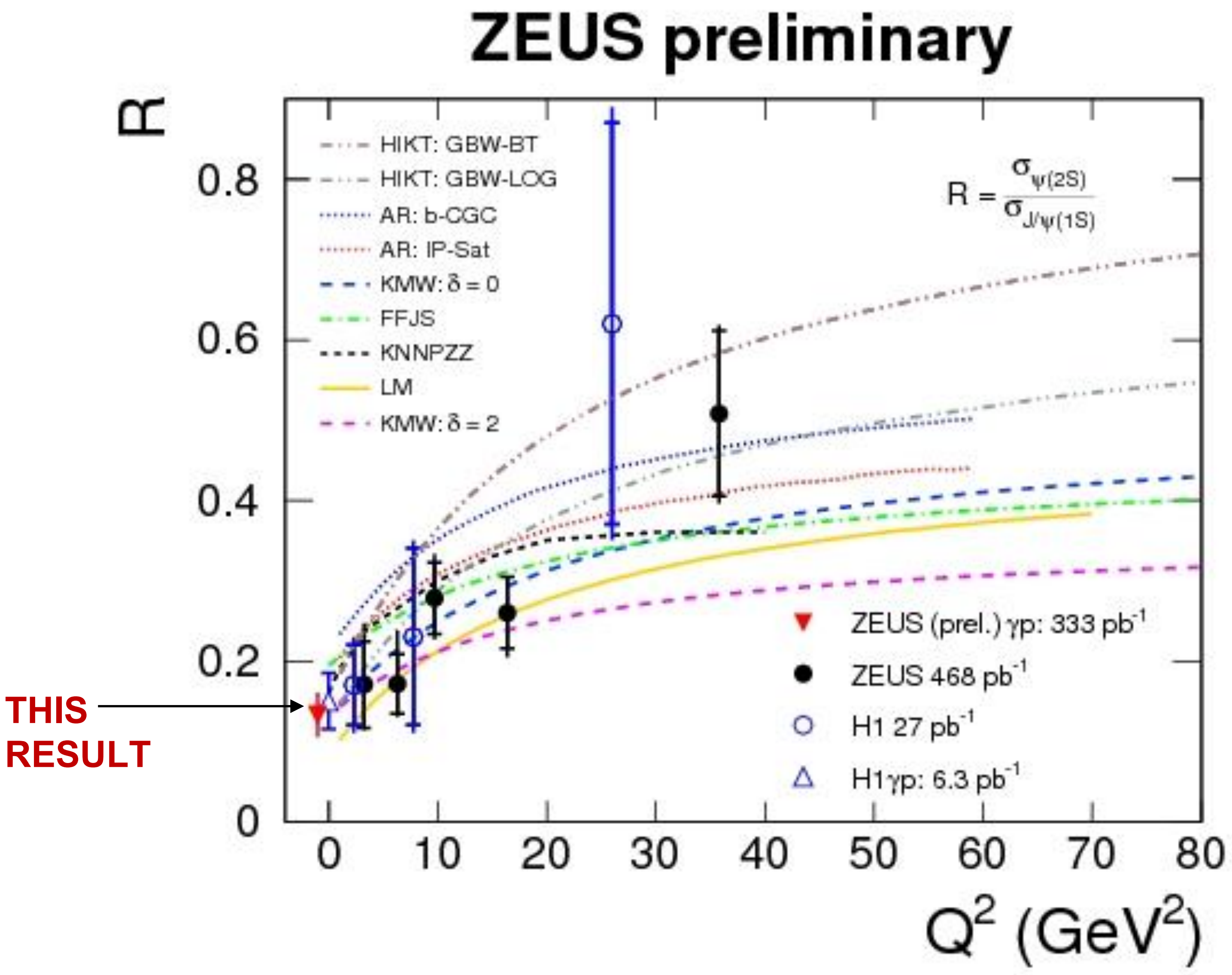

HIKT: J. Hüfner et al., PR. D 62, 094022 (2000).
KNNPZZ: B.Z. Kopeliovich et al., PR D 44, 3466 (1991), Phys. Lett. B 324, 469 (1994), Phys. Lett. B 341, 228 (1994), JETP 86, 1054 (1998).
AR: N. Armesto and A.H. Reazeian, PR D 90, 054003 (2014).
LM: T. Lappi and H.Mäntysaari, PR. C 83, 065202 (2011).
FFJS: S. Fazio et al., PR D 90, 016007 (2014).
KMW: H. Kowalski et.al., PR. D 74, 074016 (2006).

The general picture is consistent.

Conclusions

The photoproduction result fits in with others,
and the broad range of models are still relevant,
although higher Q^2 results at high precision
would be good.

H1: Diffractive production of ρ^0

Data set used (2006-2007)

Effective integrated luminosity - 1.3 pb^{-1} , Ep = 920 GeV, $\sqrt{s}$ = 319 GeV

Events with exclusive final state of one +ve and one –ve charged track only.

No further calorimeter signals unassociated with the tracks.

$p_T > 160$ MeV/c

$20^o < \theta < 160^o$

$Q^2 < 2.5$ GeV^2

Cuts on the kinematics calculated from the $\pi^+\pi^-$ final state.

$15 < W_{\gamma p} < 100$ GeV

$0 < p_T^2 < 2$ GeV^2

$0.3 < M_{\pi+\pi} < 1.5$ GeV

Model using DIFFVM MC, which includes production of ρ^0, ω, φ, ρ(1450) and ρ(1700) in Regge-based VMD production. Photon dissociation is modelled as well as the elastic process (36%)

Unfold distributions using TUnfold.

Measured $\pi^+\pi^-$ numbers of events

MC modelled background contributions are shown and are small.

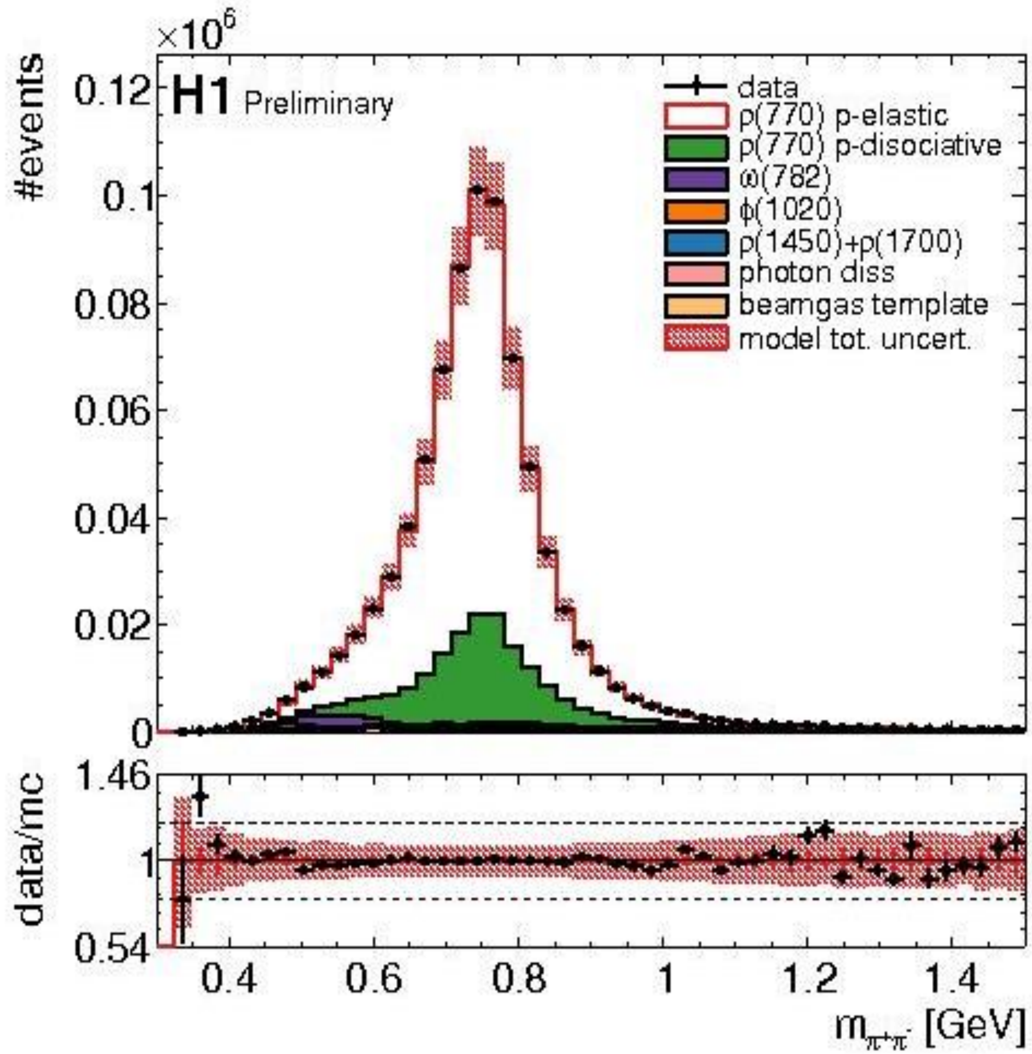

Cross section is fitted using extended Söding model incorporating relativistic Breit-Wigner shape.

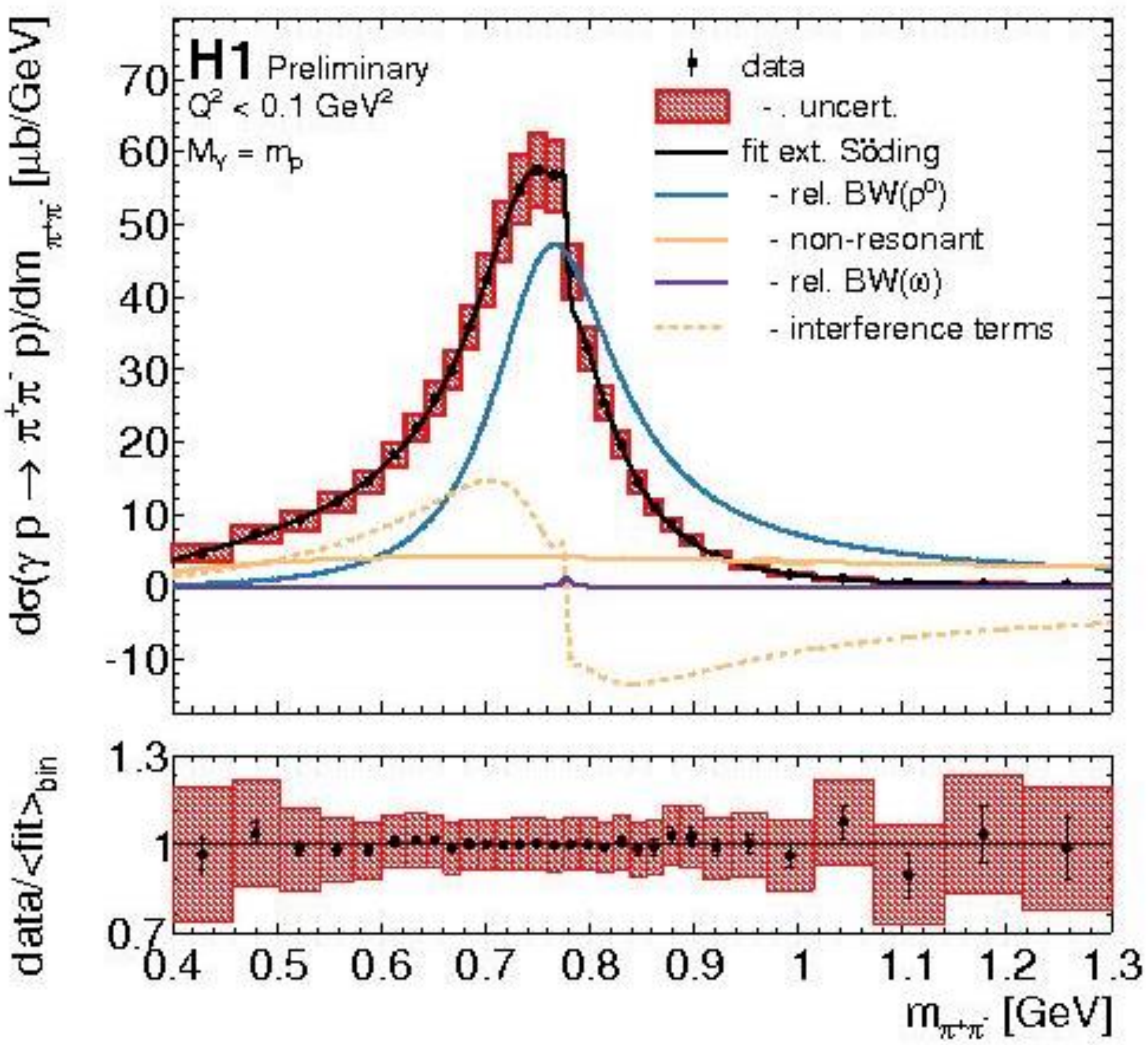

Elastic and proton-dissociative cross sections extracted using fit from model.

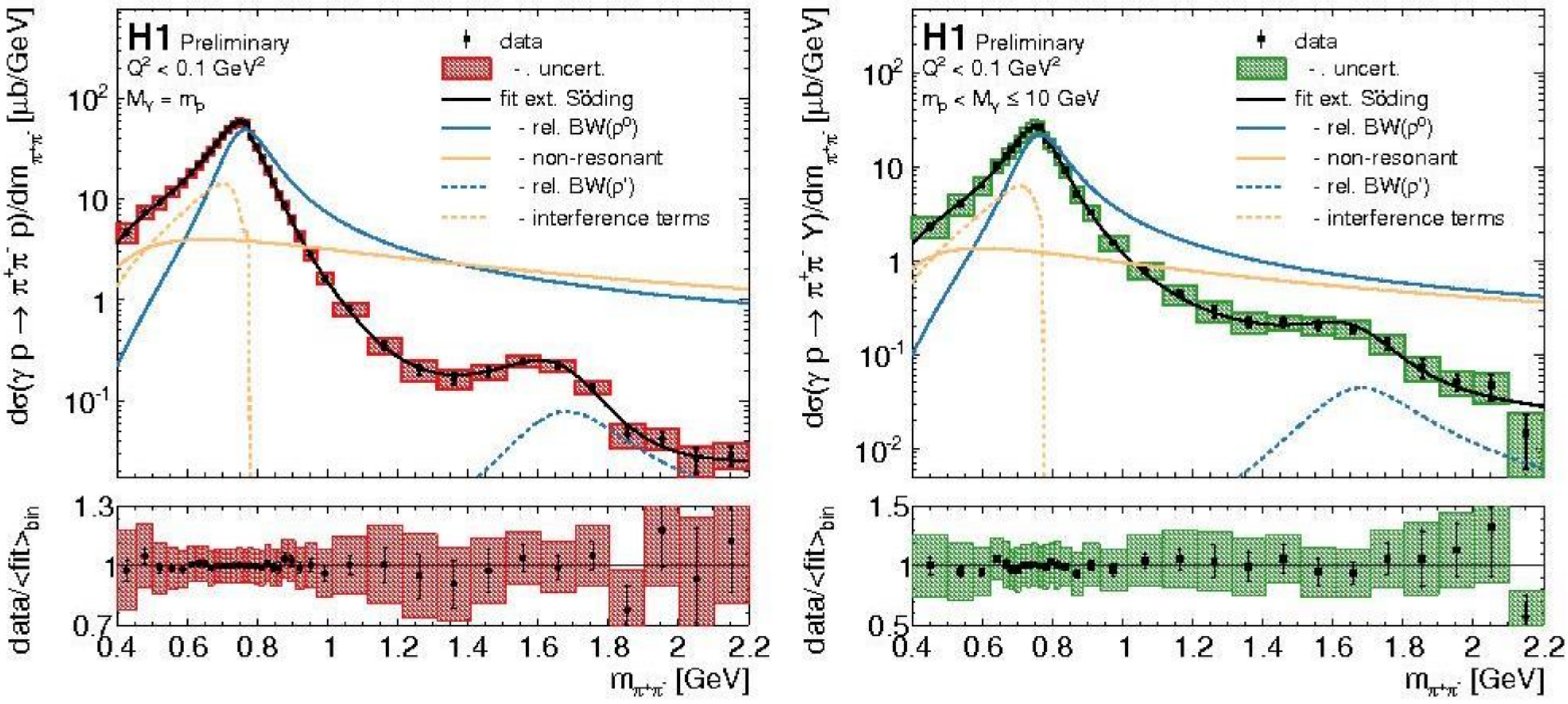

Cross section as a function of $W_{\gamma p}$.
Good consistency with other measurements.

Elastic, proton dissociative.

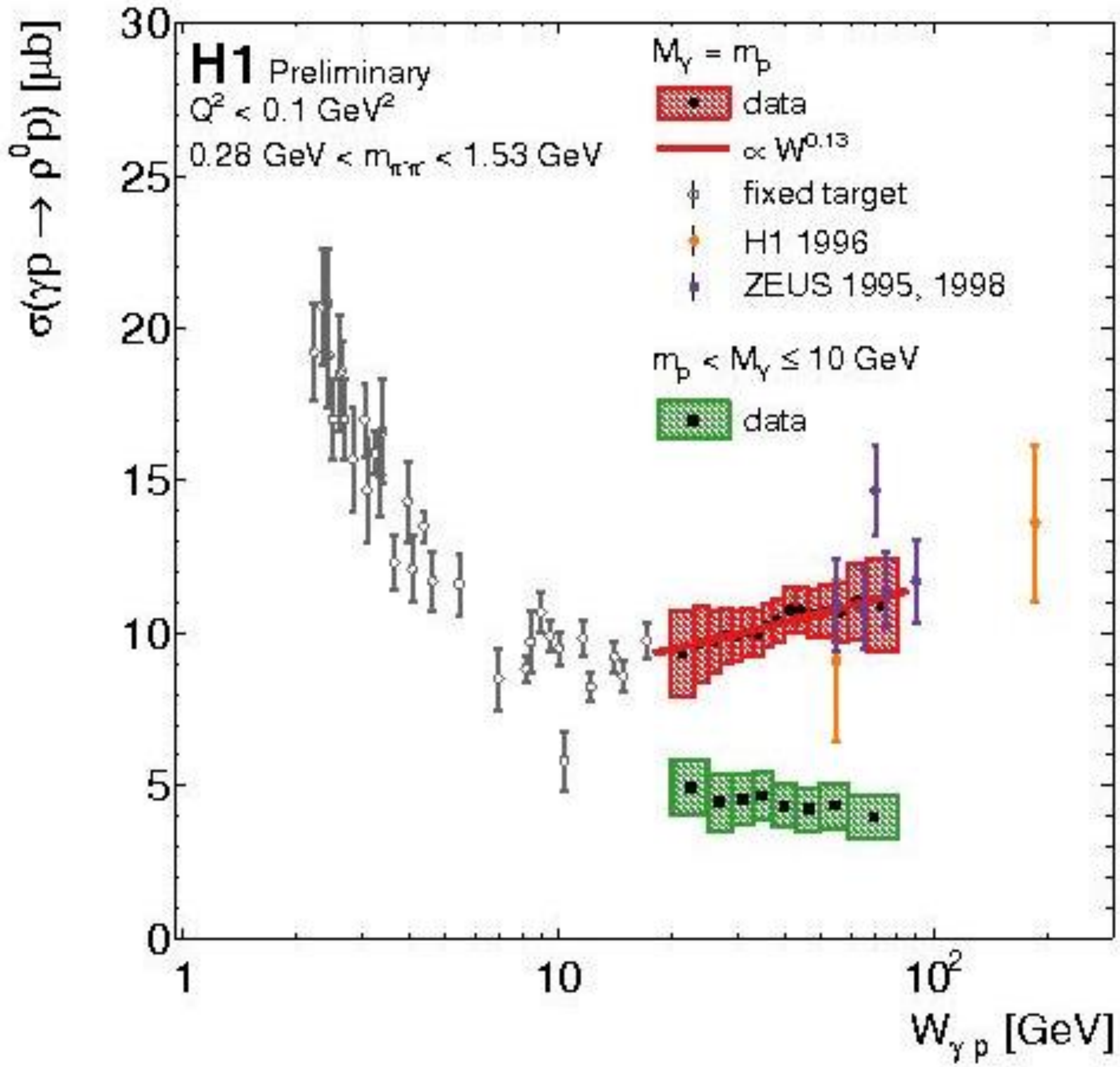

Conclusions

H1 have measured diffractive rho photoproduction and separated out the fully elastic component.

Results are consistent with other experiments over a wide range of energies.

H1: Diffractive production of $\pi^+\pi^+\pi^-\pi^-$

Two data sets were used (2006-2007)

High Energy: - 7.6 pb^{-1} ,Ep = 920 GeV, $\sqrt{s}$ = 319 GeV

Low Energy - 1.7 pb^{-1}, Ep = 460 GeV, $\sqrt{s}$ = 225 GeV

Events with exclusive final state of two +ve and two –ve charged tracks only.

$p_T > 100$ MeV/c

$20^o < \theta < 160^o$

$|t| < 1$ GeV^2 $Q^2 < 2$ GeV^2 and mass of any excited proton state < 1.6 GeV

Model the process using DIFFVM MC, which includes production of double-dissociation states of the photon and proton, $\rho(1450)$ and $\rho(1700)$ in Regge-based production model.

Detection + selection efficiency ~ 11%.

H1 total cross sections compared to previous experiments.

Very good general consistency, apart perhaps from Atiya et al.

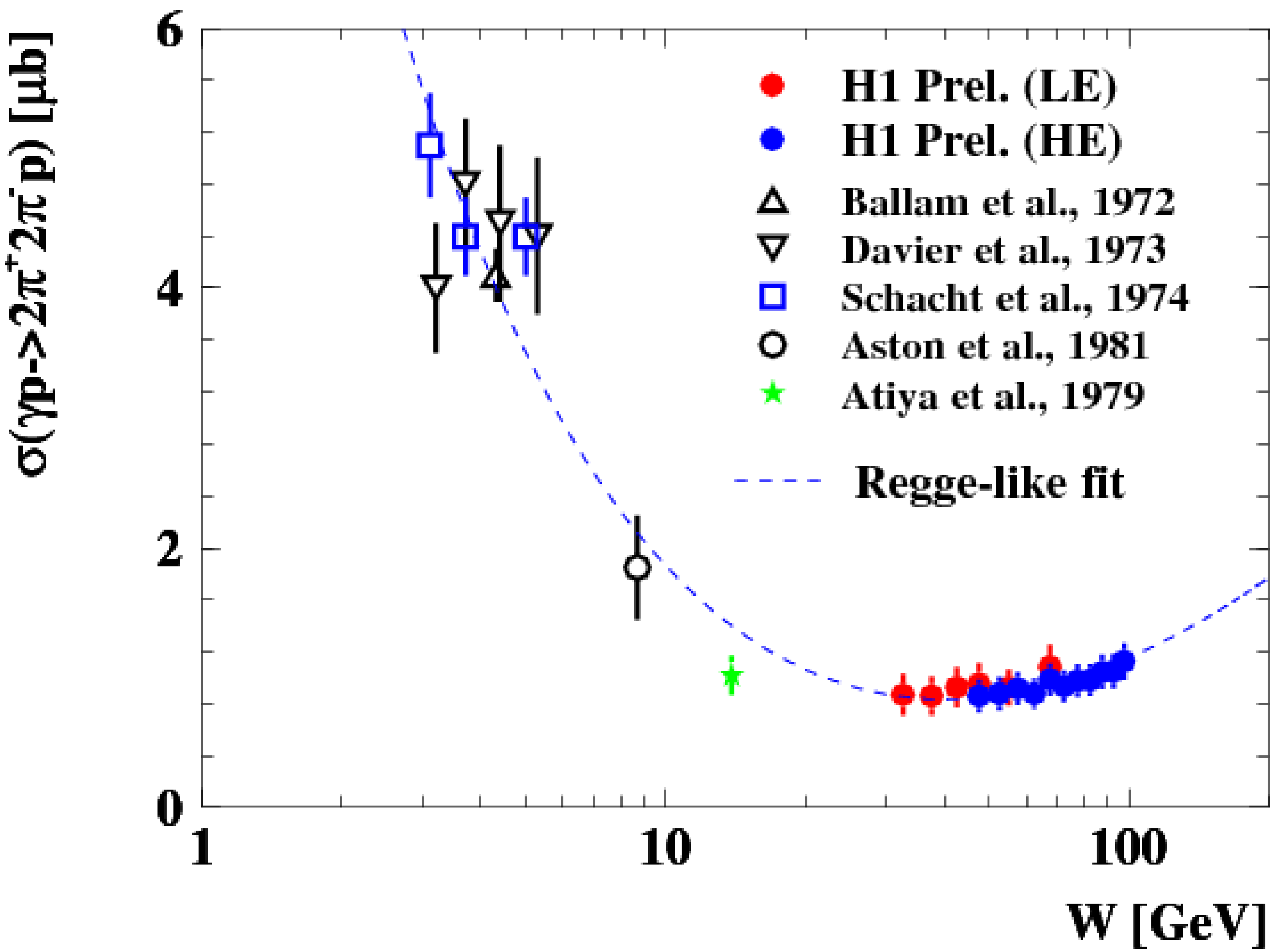

Differential cross section in p_T^2 is typical for elastic photoproduction processes.

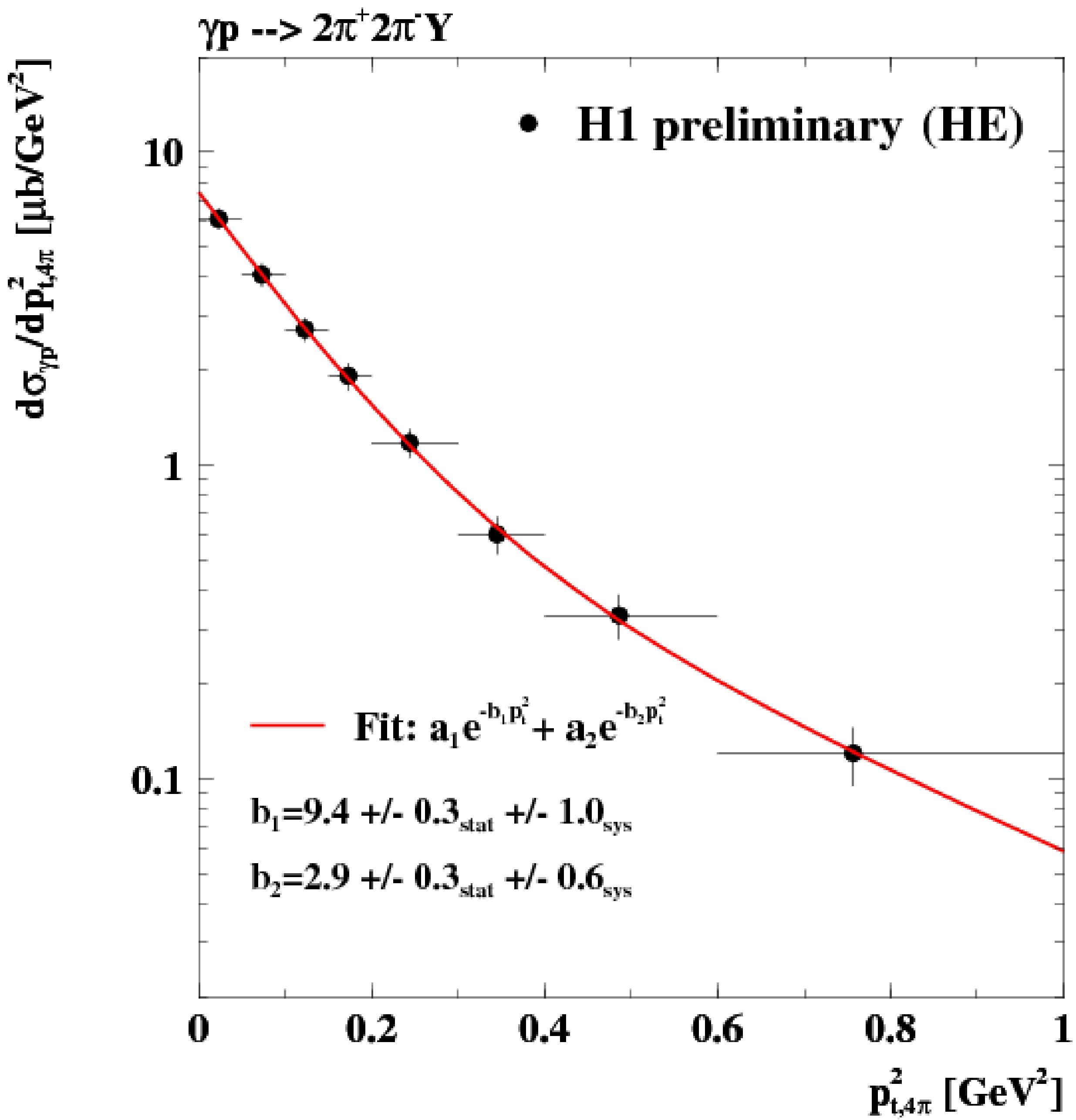

Differential cross section in $M_{4\pi}$ can be fitted with a $\rho(1600)$ model.
Cannot yet distinguish from a model with several ρ' resonances.

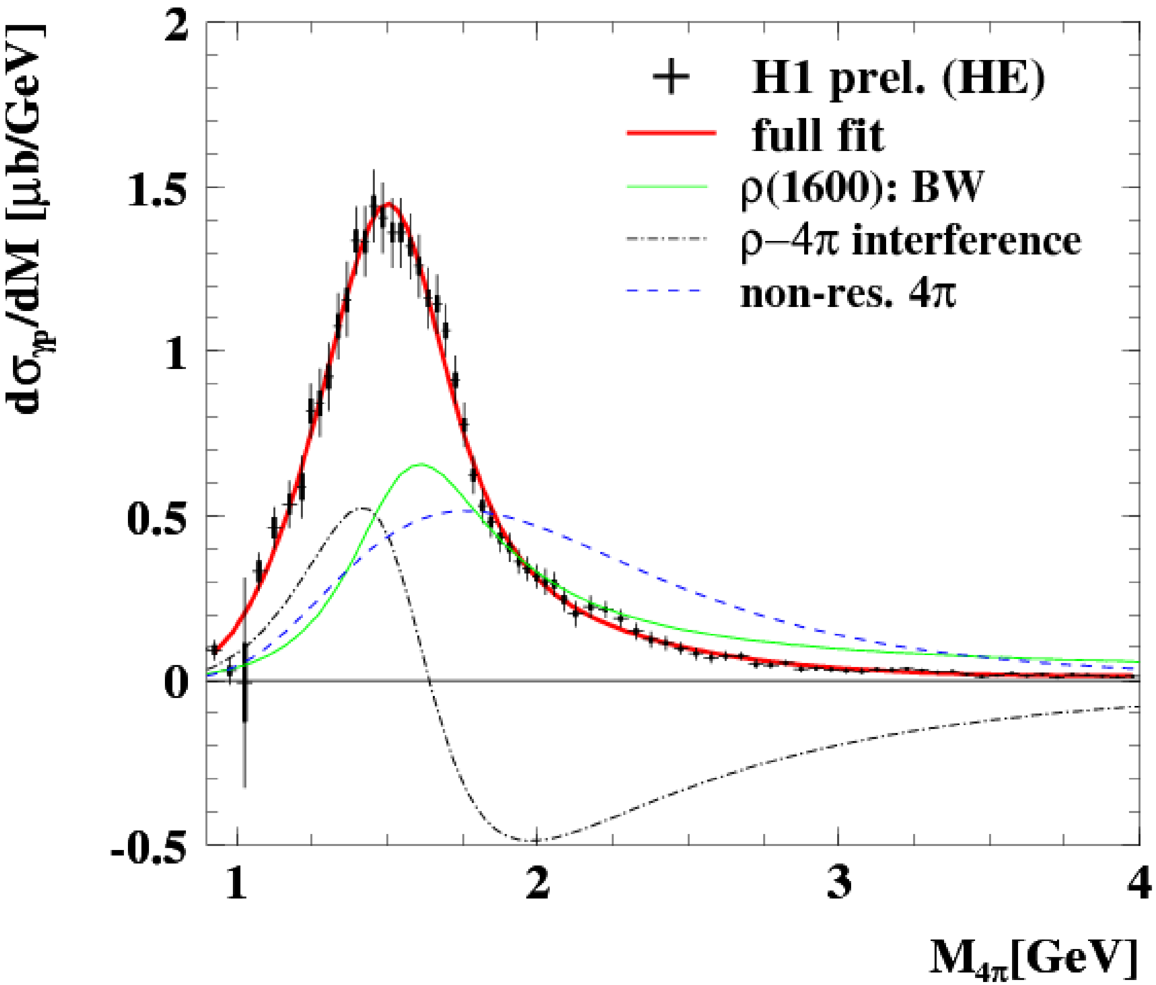

H1: A determination of Diffractive Parton Distribution Functions from inclusive diffractive deep-inelastic scattering data and diffractive dijet cross section data in next-to-next-to-leading order QCD

Previous H1 fit for diffractive PDFs was based on 1996-1997 data.
New fit uses HERA-2 inclusive data with much higher statistics.
There have also been significant theory improvements.

The approach used here assumes partonic cross sections folded with process-independent DPDFs for the diffractive production of the partons.

$$\mathrm{d}\sigma(ep \to epX) = \sum_i f_i^D(x, Q^2, x_{IP}, t) \otimes \mathrm{d}\sigma^{ie}(x, Q^2)$$

There is a Pomeron term and a much smaller Reggeon term.

$$f_i^D(z, \mu^2, x_{I\!P}, t) = f_{I\!P/p}(x_{I\!P}, t) f_{i/I\!P}(z, \mu^2) + n_{I\!R} f_{I\!R/p}(x_{I\!P}, t) f_{i/I\!R}(z, \mu^2)$$

For further details see talk by Radek Žlebčík at the 2019 DIS workshop.

Previous H1 fit for diffractive PDFs was based on 1996-1997 data.
New fit uses HERA-2 inclusive data with much higher statistics.

Data set [ref.]	$\sqrt{s}$ [GeV]	int. $\mathcal{L}$ [pb^{-1}]	DIS kinematic range
H1comb-LRG	319	336.6	$8.5 < Q^2 < 1600\,\mathrm{GeV}^2$
H1-LowE-252	252	5.2	$8.5 < Q^2 < 44\,\mathrm{GeV}^2$
H1-LowE-225	225	8.5	$8.5 < Q^2 < 44\,\mathrm{GeV}^2$

The combined “large rapidity gap” data set includes HERA-1 and HERA-2 data taken from 1997 to 2007.

In addition, several sets of diffractive dijet data were used:

Data Set	$\mathcal{L}$ [pb^{-1}]	DIS range	Dijet range	Diffractive range
H1 LRG (HERA 2) [5]	290 (~15000ev)	$4 < Q^2 < 100\,\mathrm{GeV}^2$ $0.1 < y < 0.7$	$p_T^{*,\mathrm{jet1}} > 5.5\,\mathrm{GeV}$ $p_T^{*,\mathrm{jet2}} > 4.0\,\mathrm{GeV}$ $-1 < \eta_{\mathrm{lab}}^{\mathrm{jet}} < 2$	$x_{\mathbb{P}} < 0.03$ $\|t\| < 1\,\mathrm{GeV}^2$ $M_Y < 1.6\,\mathrm{GeV}$

These represent a subset of the LRG inclusive data and were analysed in a way that presents more detailed kinematic information than the inclusive selection.

Results from the fits are shown in following slides.

Data set	process	χ^2/n_{data}
H1comb-LRG	inclusive NC DDIS	192/191
H1-LowE-225	inclusive NC DDIS	19/12
H1-LowE-252	inclusive NC DDIS	10/13
H1 LRG (HERA 2)	dijet production	12/15
all		235/231
		$[n_{\mathrm{dof}} = 223]$

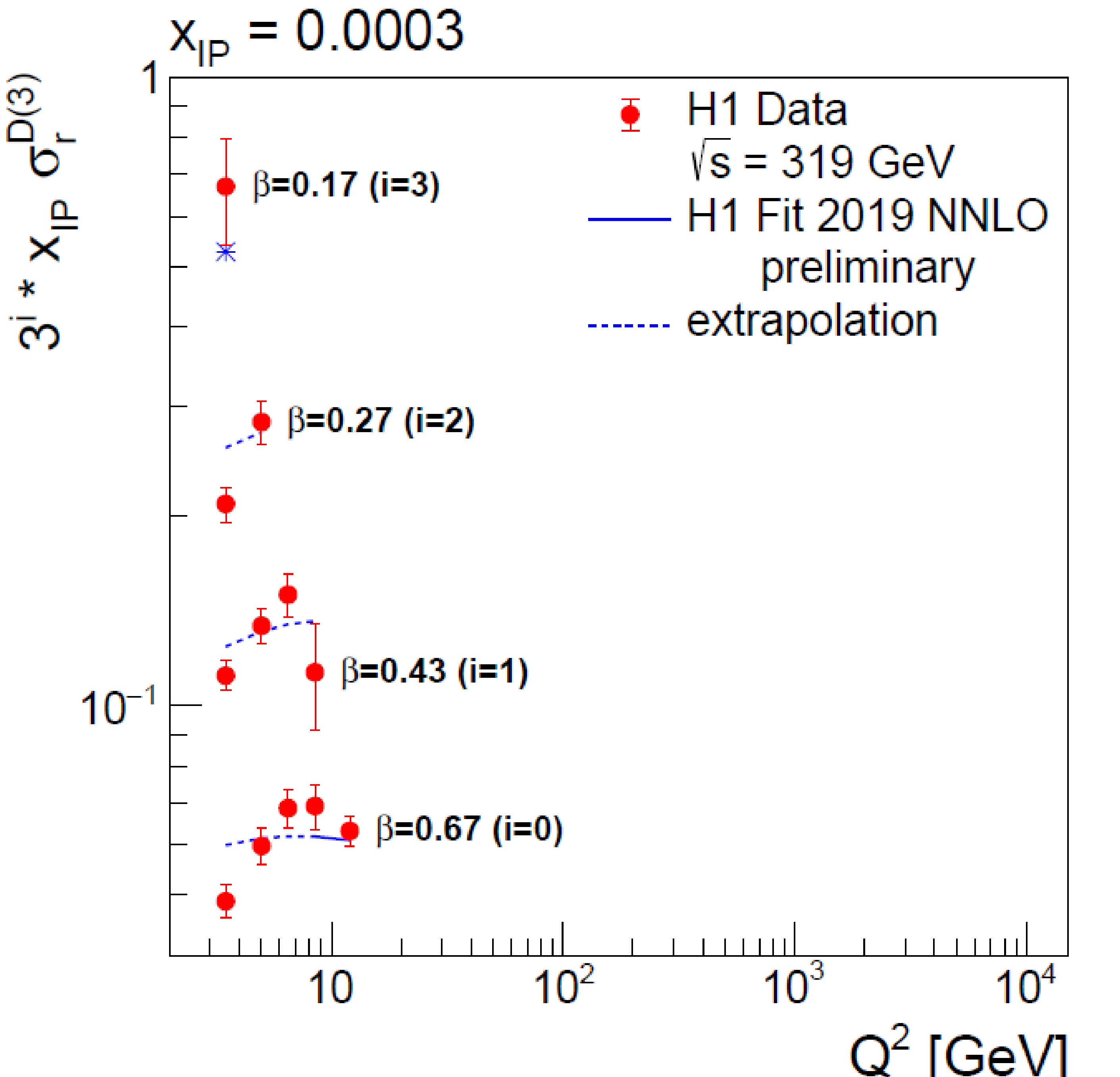

x_{IP} = 0.0003
$3^i * x_{IP}\, \sigma_r^{D(3)}$
1
10^{-1}
10
10^2
10^3
10^4
Q^2 [GeV]
H1 Data
$\sqrt{s}$ = 319 GeV
H1 Fit 2019 NNLO
preliminary
extrapolation
β=0.17 (i=3)
β=0.27 (i=2)
β=0.43 (i=1)
β=0.67 (i=0)

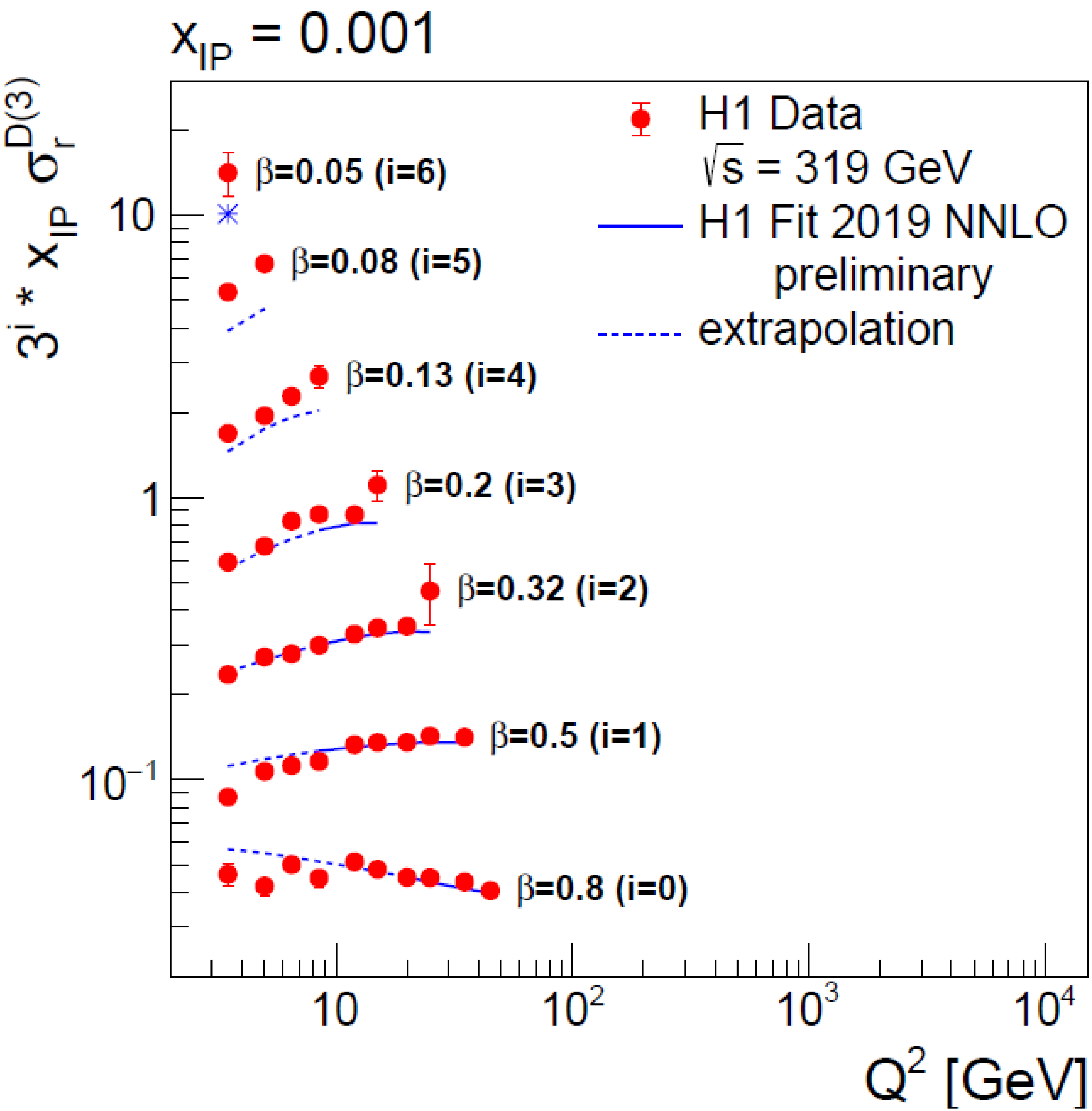

x_{IP} = 0.001
$3^i * x_{IP}\,\sigma_r^{D(3)}$
10
1
10^{-1}
10
10^2
10^3
10^4
Q^2 [GeV]
β=0.05 (i=6)
β=0.08 (i=5)
β=0.13 (i=4)
β=0.2 (i=3)
β=0.32 (i=2)
β=0.5 (i=1)
β=0.8 (i=0)
H1 Data
$\sqrt{s}$ = 319 GeV
H1 Fit 2019 NNLO preliminary
extrapolation

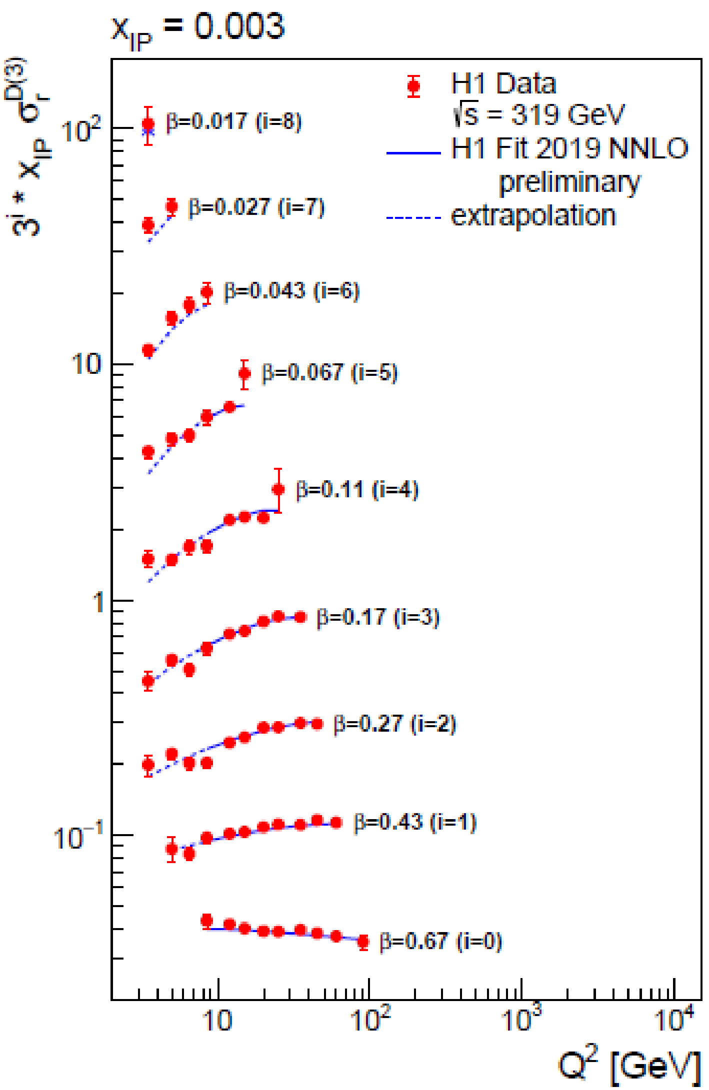

x_{IP} = 0.003
$3^i * x_{IP}\, \sigma_r^{D(3)}$
H1 Data
$\sqrt{s}$ = 319 GeV
H1 Fit 2019 NNLO preliminary
extrapolation
β=0.017 (i=8)
β=0.027 (i=7)
β=0.043 (i=6)
β=0.067 (i=5)
β=0.11 (i=4)
β=0.17 (i=3)
β=0.27 (i=2)
β=0.43 (i=1)
β=0.67 (i=0)
Q^2 [GeV]

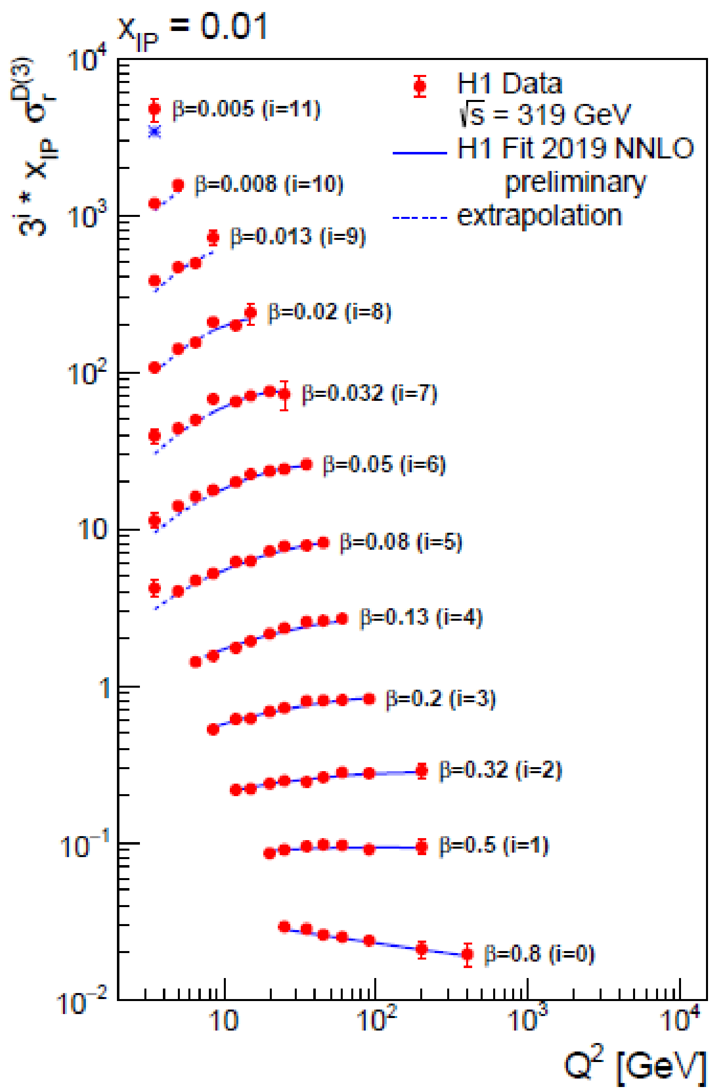

x_{IP} = 0.01
$3^i * x_{IP}\, \sigma_r^{D(3)}$
H1 Data
$\sqrt{s}$ = 319 GeV
H1 Fit 2019 NNLO preliminary
extrapolation
β=0.005 (i=11)
β=0.008 (i=10)
β=0.013 (i=9)
β=0.02 (i=8)
β=0.032 (i=7)
β=0.05 (i=6)
β=0.08 (i=5)
β=0.13 (i=4)
β=0.2 (i=3)
β=0.32 (i=2)
β=0.5 (i=1)
β=0.8 (i=0)
Q^2 [GeV]

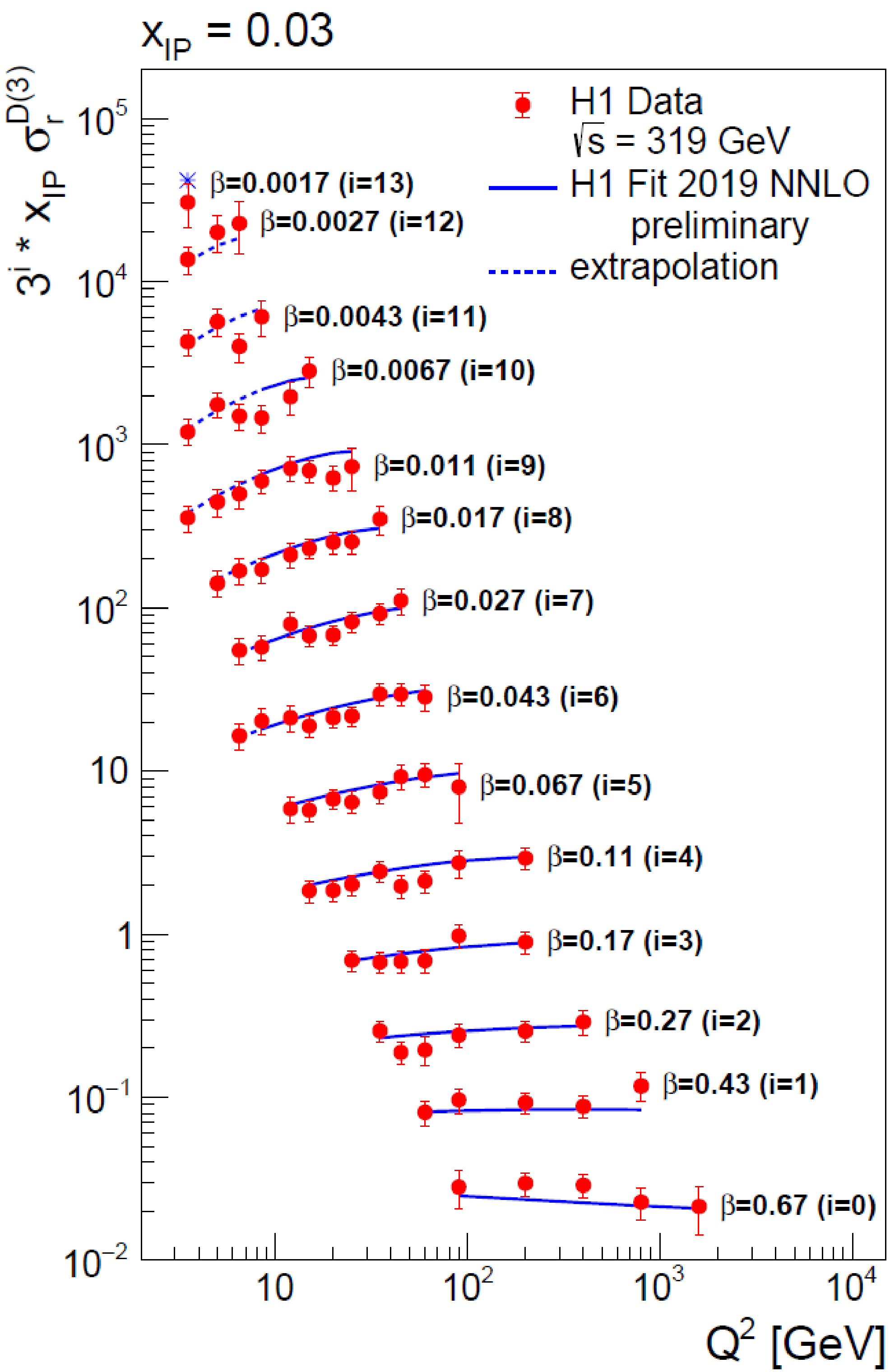

x_{IP} = 0.03
$3^i * x_{IP}\ \sigma_r^{D(3)}$
H1 Data
$\sqrt{s}$ = 319 GeV
H1 Fit 2019 NNLO preliminary
extrapolation
β=0.0017 (i=13)
β=0.0027 (i=12)
β=0.0043 (i=11)
β=0.0067 (i=10)
β=0.011 (i=9)
β=0.017 (i=8)
β=0.027 (i=7)
β=0.043 (i=6)
β=0.067 (i=5)
β=0.11 (i=4)
β=0.17 (i=3)
β=0.27 (i=2)
β=0.43 (i=1)
β=0.67 (i=0)
Q^2 [GeV]

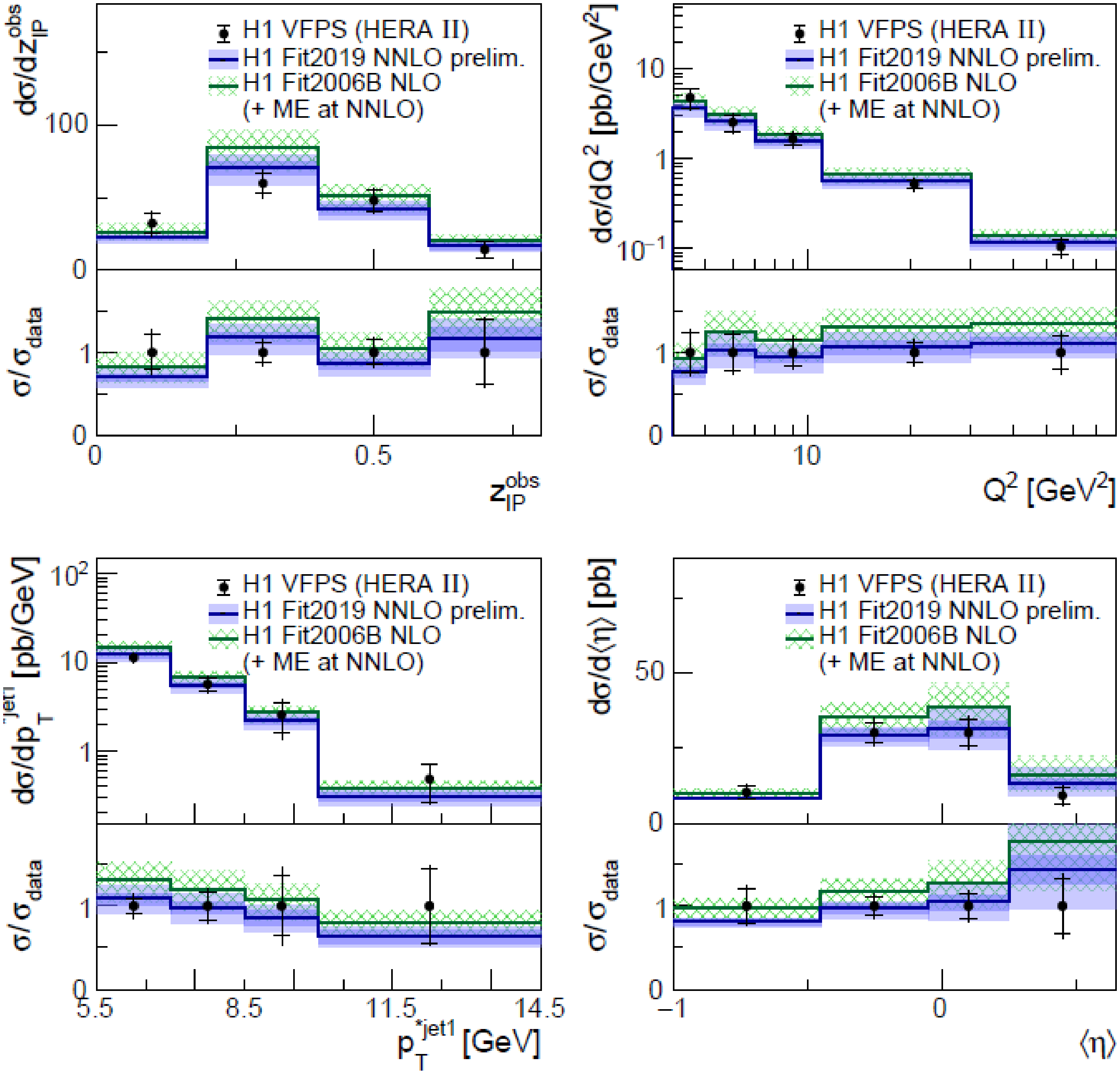
H1 VFPS (HERA II)
H1 Fit2019 NNLO prelim.
H1 Fit2006B NLO
(+ ME at NNLO)
$d\sigma/dz_{IP}^{obs}$
σ/σ_{data}
z_{IP}^{obs}
$d\sigma/dQ^2$ [pb/GeV^2]
Q^2 [GeV^2]
$d\sigma/dp_T^{*jet1}$ [pb/GeV]
p_T^{*jet1} [GeV]
$d\sigma/d\langle\eta\rangle$ [pb]
$\langle\eta\rangle$

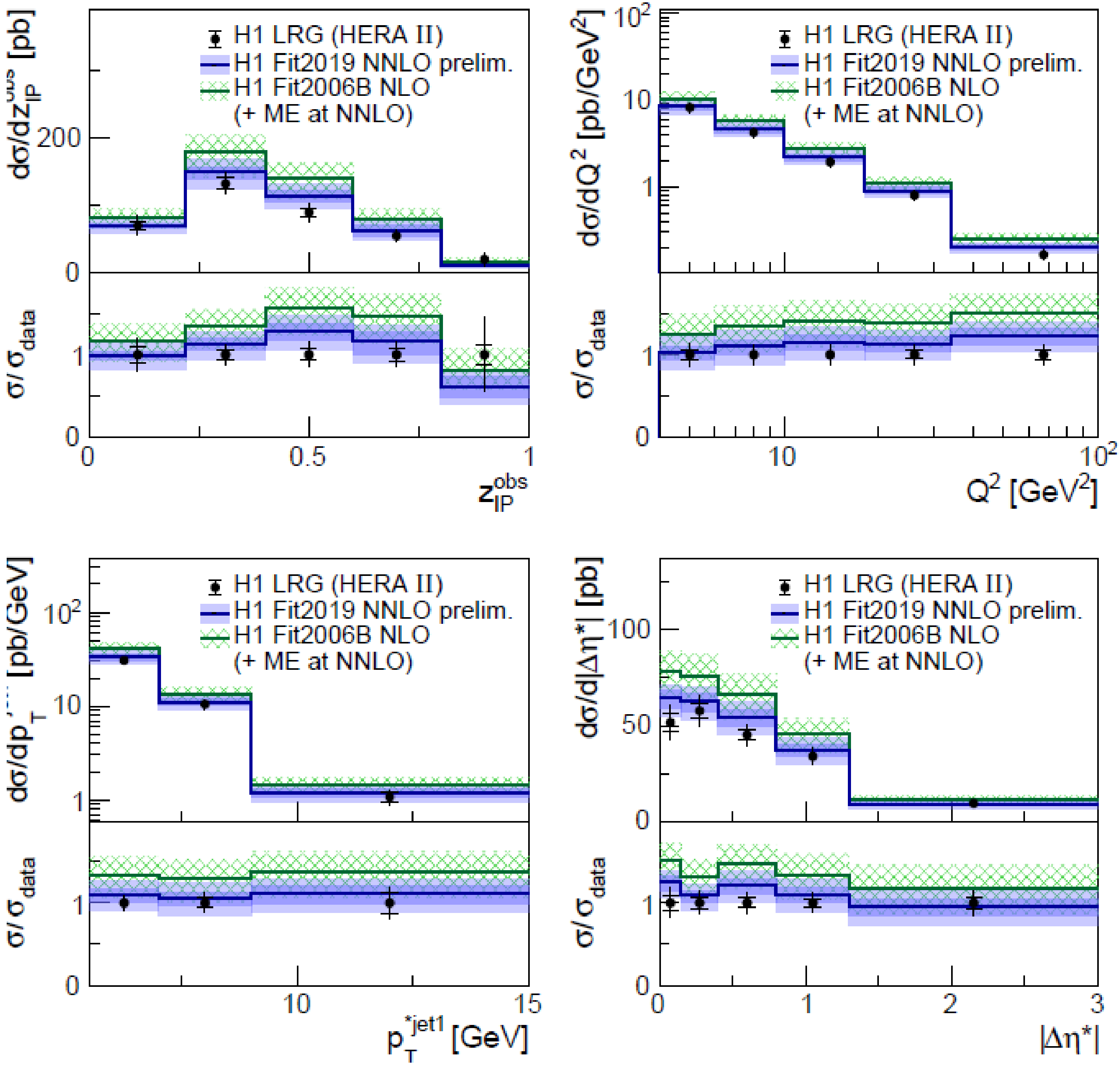
H1 LRG (HERA II)
H1 Fit2019 NNLO prelim.
H1 Fit2006B NLO
(+ ME at NNLO)
$d\sigma/dz_{IP}^{obs}$ [pb]
σ/σ_{data}
z_{IP}^{obs}
$d\sigma/dQ^2$ [pb/GeV^2]
Q^2 [GeV^2]
$d\sigma/dp_T^{*jet1}$ [pb/GeV]
p_T^{*jet1} [GeV]
$d\sigma/d|\Delta\eta^*|$ [pb]
$|\Delta\eta^*|$

Comments

The fit is good over the fitted region, and agrees well with a number of parameters. It extrapolates well in some regions but not in others..

It is found that

- The NNLO DPDF has a lower gluon contribution than the earlier NLO version

- The dijet data are well fitted by both versions and are compatible with the inclusive data

- This supports the assumption of factorisation.

Summary

Still a modest but steady flow of results from HERA.

ZEUS have measured isolated ("prompt") photons in

- diffractive photoproduction, for the first time with an accompanying jet.
- Deep Inelastic Scattering, measuring new combinations of variables

Also, the $\psi(2S)$ to J/ψ cross-section ratio in photoproduction

H1 have measured

- The elastic rho cross section in photoproduction
- The diffractive production of $\pi^+\pi^+\pi^-\pi^-$

Also, a new PDF fit to diffractive DIS production has been performed.

There are other results, but not for this conference!

Backups

Some comparisons with earlier results. Always a need to scale up the LO theory

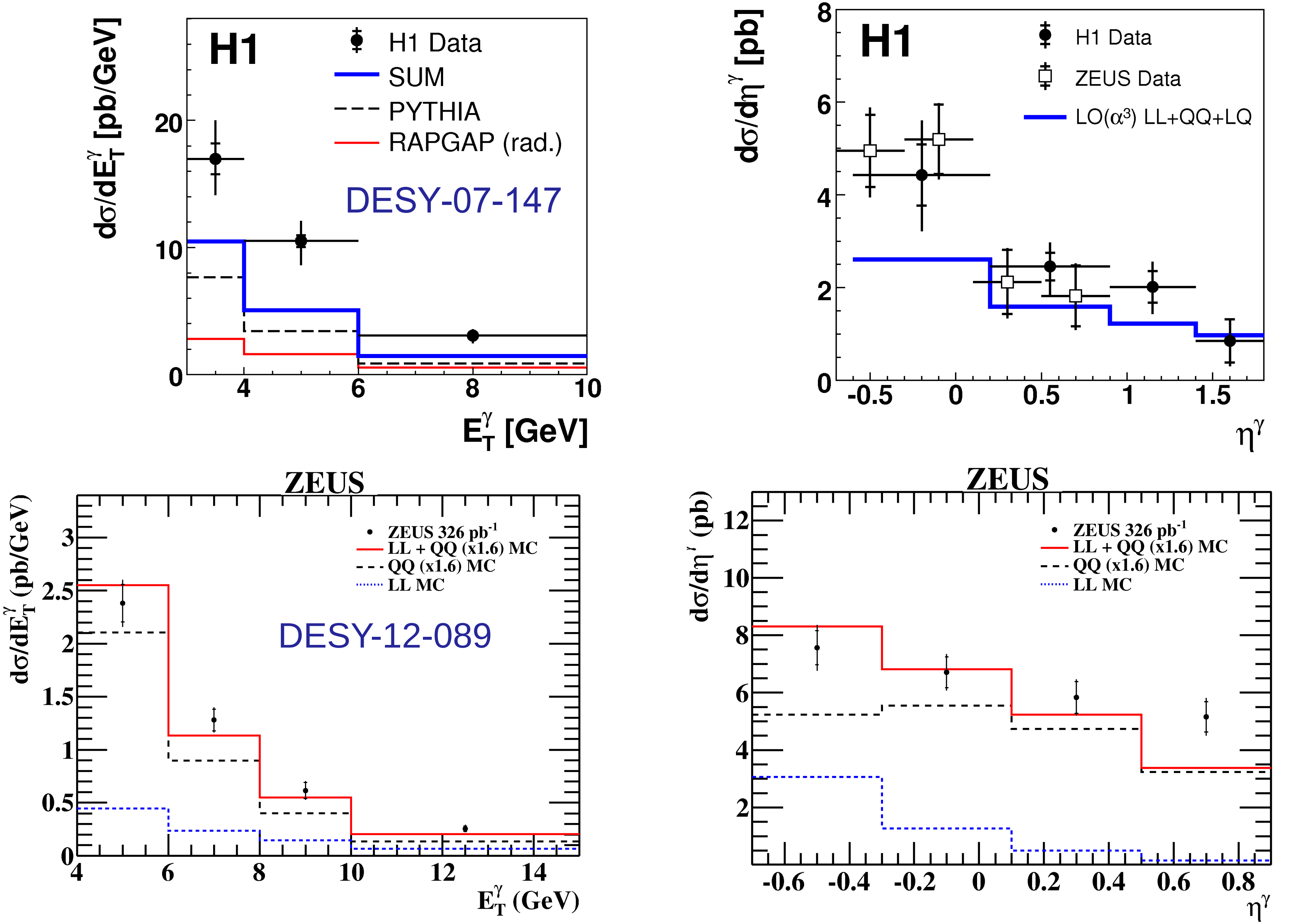

Plot z_{IP}^{meas} and compare with Rapgap

Shape does not agree.

An excess is seen in the top bin.

Can reweight Rapgap to describe the shape.

Unreweighted Rapgap here normalised to $z_{IP}^{meas} < 0.9$ data. Otherwise, unless stated, Rapgap is normalised to the full plotted range of data.

The η_{max} distribution is described better by the reweighted Rapgap.

Red histogram shows what 10% of non-diffractive Pythia photoproduction (subject to present cuts) would look like. (Not added into the Rapgap.)

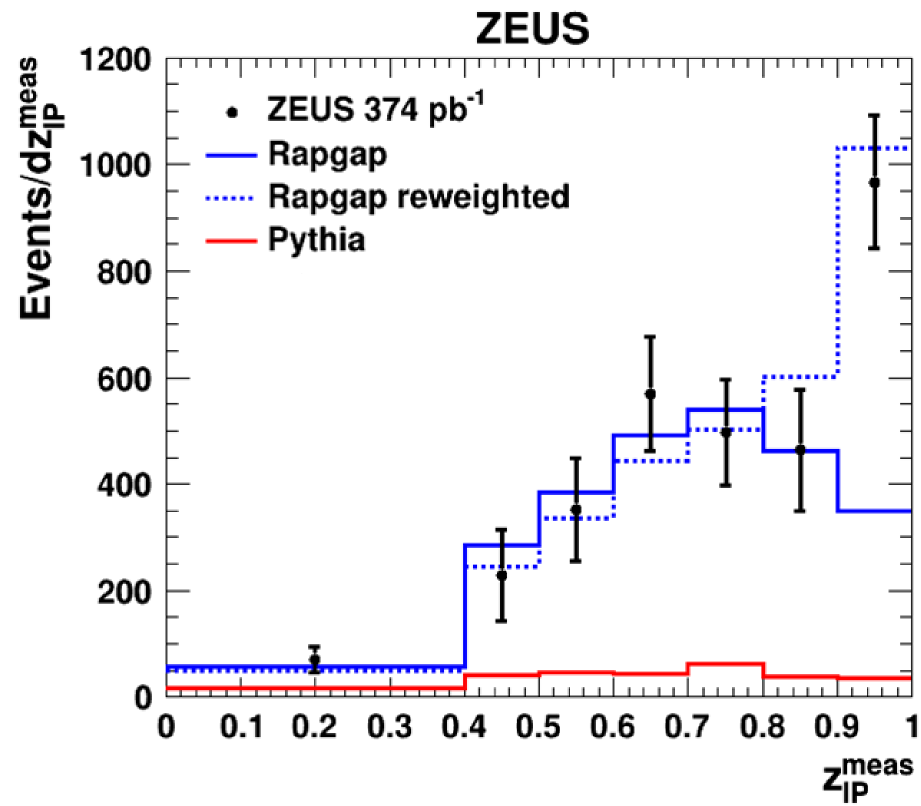

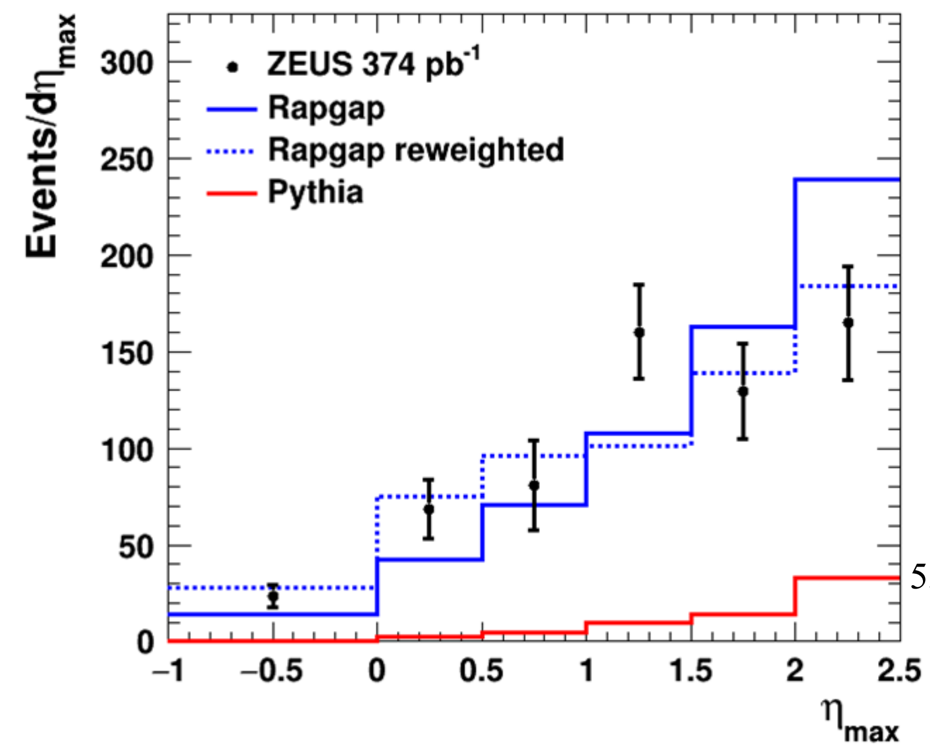

Photon candidates: groups of signals in cells in the BEMC.
Each has a Z-position, Z_{CELL}. E-weighted mean of Z_{CELL} is Z_{Mean}.

Task: to separate photons from background
of candidates from photon decays of neutral mesons.

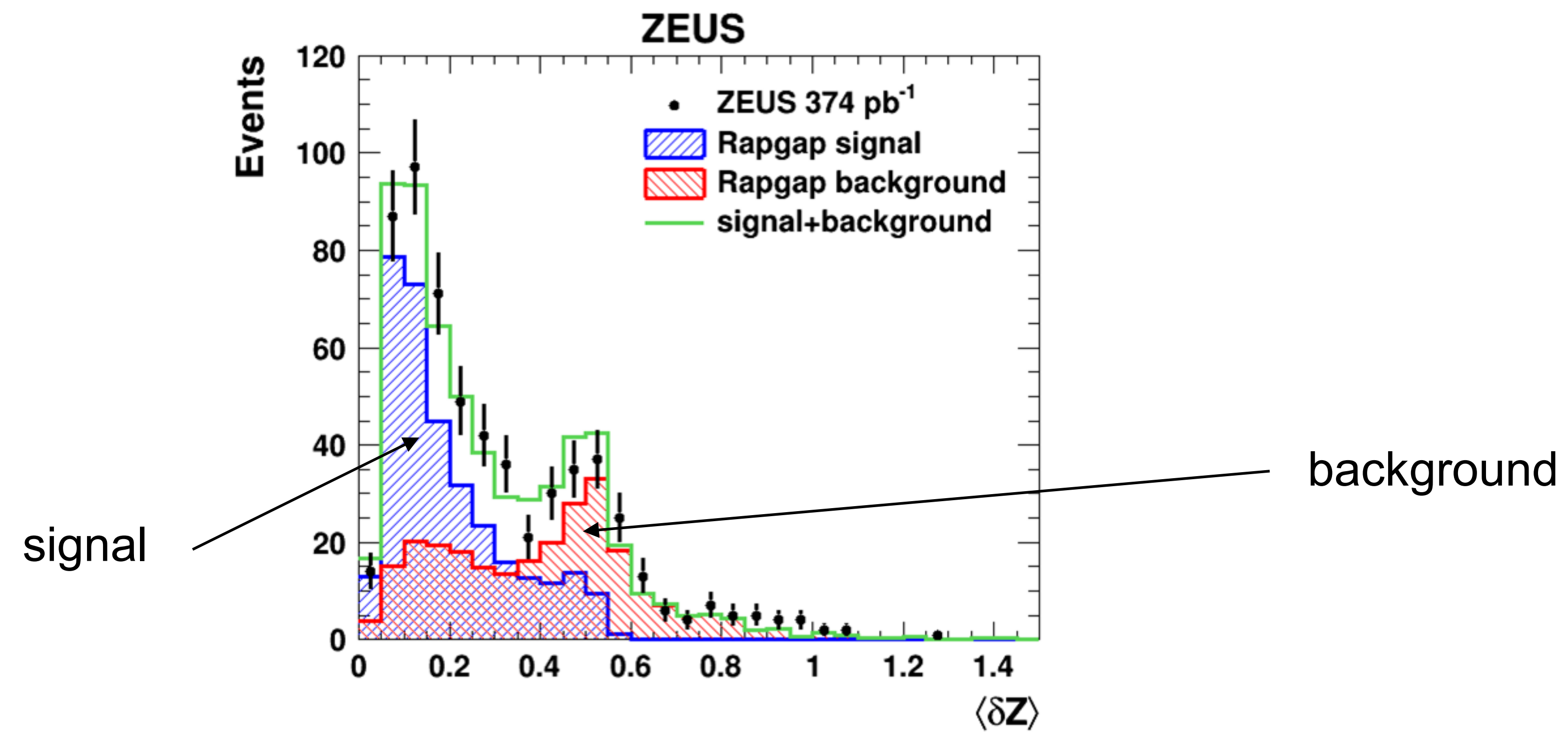

$\langle dZ \rangle$ = E-weighted mean of $|Z_{CELL} - Z_{Mean}|$.

Peaks correspond to photon and π^0 signals, other background is η + multi-π^0.

In each bin of each measured physical quantity, fit for **photon signal** + hadronic bgd.

etamax distribution for HERA-2.

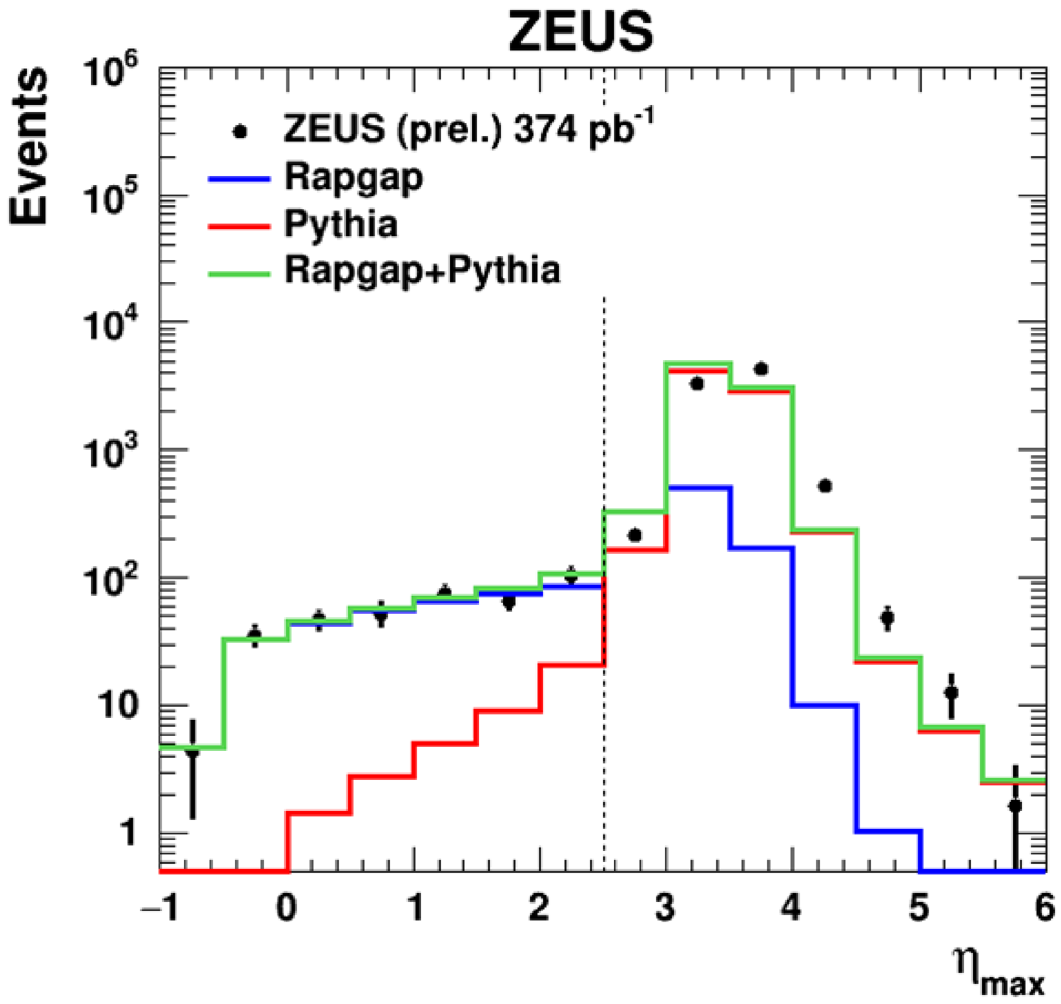

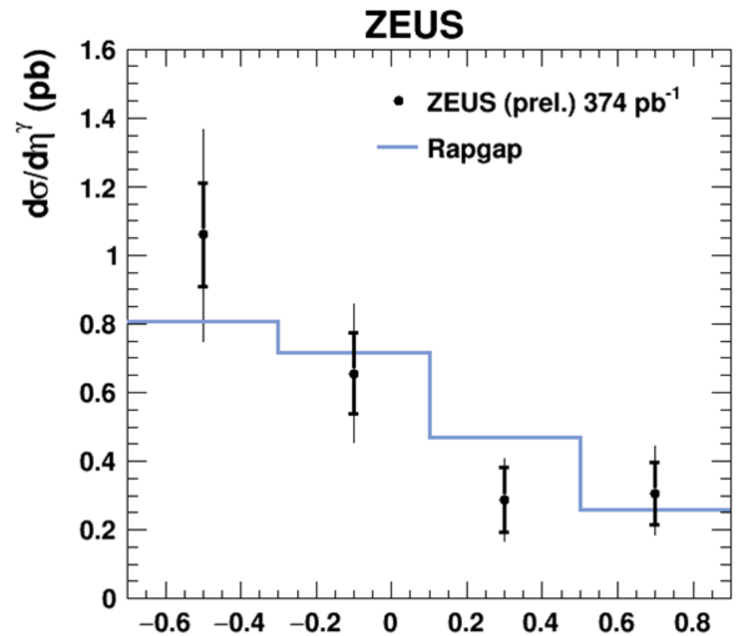

Inclusive photon pseudorapidity

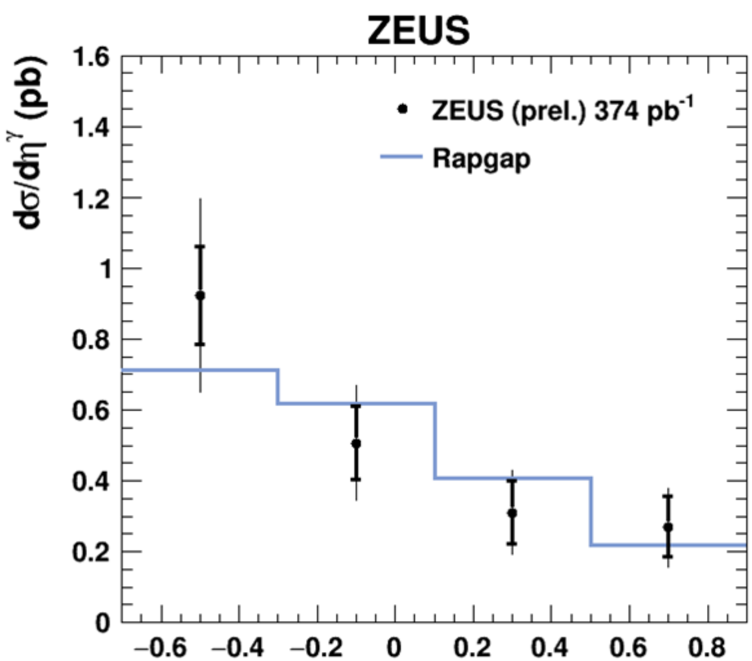

Photon + jet

Compare diffractive photon distribution with those from nondiffractive process.

Diffractive more resembles direct but seems slightly more forward.

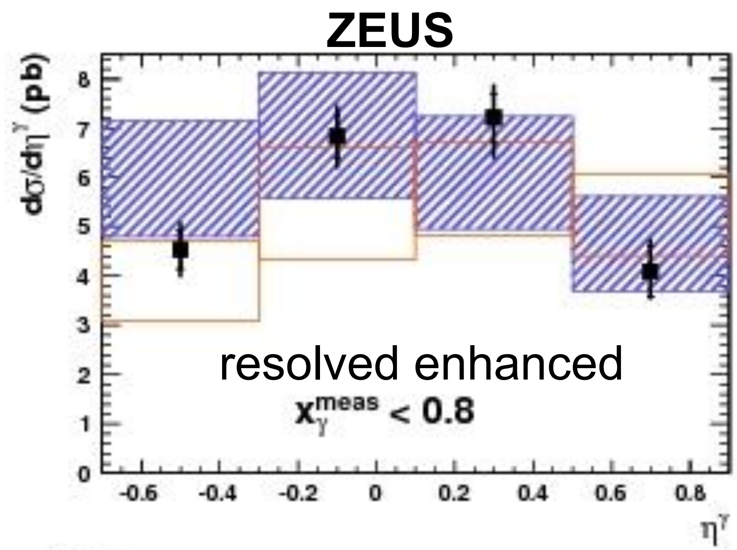

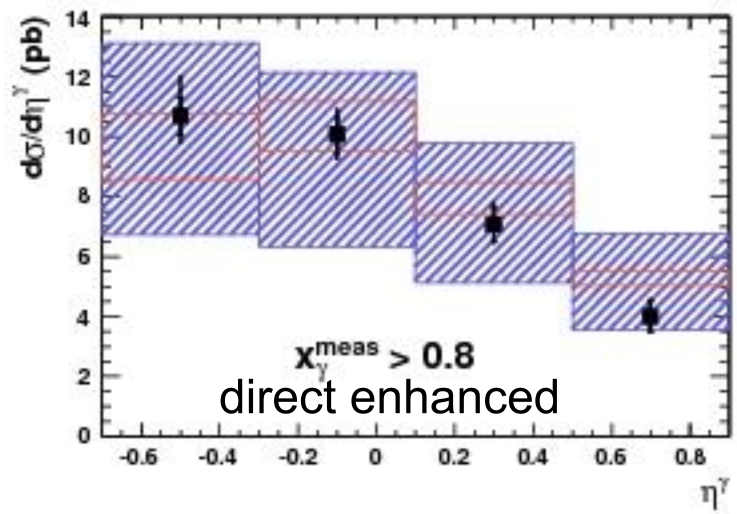

Compare diffractive distribution with that for nondiffractive photoproduction:

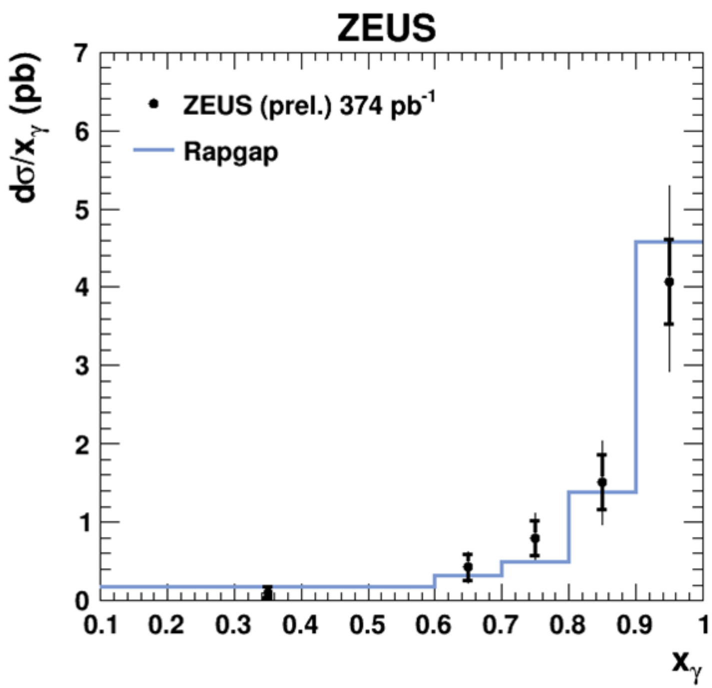

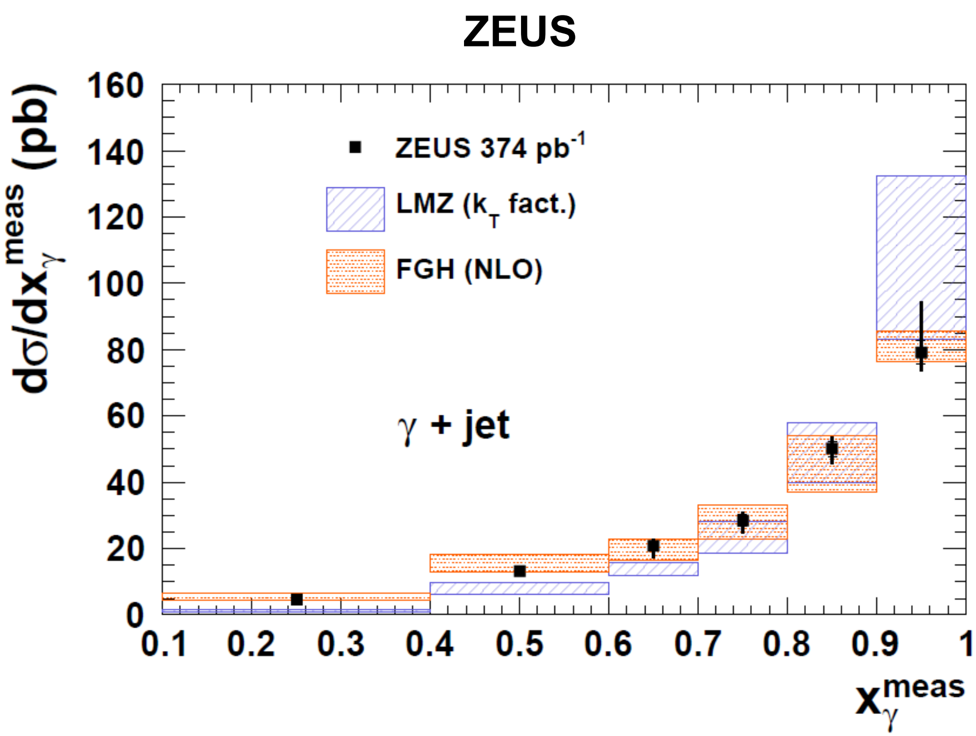

The diffractive process (left) is more strongly direct-dominated than the photoproduction (right).
Rapgap gives a good description.